Supplementary Information for

Host-guest directed construction of phenothiazine supramolecular frameworks with enhanced oxygen reactivity for visible-light photocatalysis

Xian-Ya Yao,‡ Jin-Ru Chen,‡ Hui Liu, Zhe Lian,* Wen-Qiang Liu* and Ling-Bao Xing*

School of Chemistry and Chemical Engineering, Shandong University of Technology, Zibo 255000, P. R. China.

E-mail: lianzchem@bnu.edu.cn; liuwenqiang13@mail.ipc.ac.cn; lbxing@sdut.edu.cn.

‡These authors contributed equally to this work.

Contents

1 Experimental section

1.1 Materials

Unless specifically mentioned, all chemicals are commercially available and were used as received.

1.2 Characterization

^{1}H NMR spectra was recorded on a Bruker Advance 400 spectrometer (400 MHz) at 298 K, and the chemical shifts (δ) were expressed in ppm and J values were given in Hz. UV-vis spectra were obtained on a Shimadzu UV-1601PC spectrophotometer in a quartz cell (light path 10 mm) at 298 K. Steady-state fluorescence measurements were carried out using a Hitachi 4500 spectrophotometer. Dynamic light scattering (DLS) and zeta potential are measured on Malvern Zetasizer Nano ZS90. Scanning electron microscopy (SEM) images were obtained on a Hitachi SU8010 operating at 5 kV. Samples for SEM measurements were prepared by placing the dry powder onto conductive adhesive tape attached to a sample stub, followed by sputter-coating with gold. Transmission electron microscopy (TEM) images were obtained on a JEM 2100 operating at 120 kV. Samples for TEM measurements were prepared by dropping the mixture aqueous solution on carbon-coated copper grid (300 mesh) and drying by slow evaporation. Atomic force microscopy (AFM) images were obtained on a Bruker Multimode 8 in tapping mode. Samples for AFM measurements were prepared by dropping the mixture aqueous solution on a silicon wafer and drying by slow evaporation. The photocatalytic reaction was performed on WATTCAS Parallel Photocatalytic Reactor (WP-TEC-HSL) with 18W COB LED. X-ray diffraction (XRD) patterns were conducted using a Bruker D8 Advance diffraction with Cu Kα radiation (λ = 1.5418 Å). The interplanar crystal spacing was calculated by the Bragg equation ($2d \sin \theta = n\lambda$). The electron paramagnetic resonance (EPR) spectra of reactive oxygen species and spin signals were measured on the Bruker-BioSpin E500 spectrometer.

1.3 Typical procedure for the synthesis of 2-phenylbenzothiazole

2-aminobenzenethiol 1 (0.2 mmol) and benzaldehyde 2 (0.2 mmol) were added to the newly prepared 3PPTZ-CB[8] (0.5 mol%, 3.0 mL, [3PPTZ] = 3.0×10^{-5} M, [CB[8]] = 4.5×10^{-5} M) in H_2O. After irradiating with a blue LEDs (18 W, 430-440 nm) at room temperature for 3 h, the mixture was extracted with dichloromethane, and the organic layer was dried with anhydrous Na_2SO_4. Then the organic solvent was removed in vacuo and purified by column chromatography with petroleum ether/ethyl acetate to afford the products.

1.4 Synthetic route

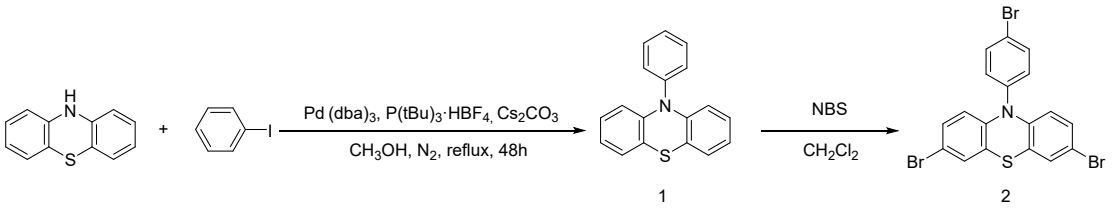

Scheme S1. Synthetic route of **compound 1** and **2**.

Synthesis of compound 1: In a 100 mL round-bottom flask, 10H-phenothiazine (0.199 g, 1.0 mmol) and iodobenzene (0.111 mL, 1.0 mmol) were added to 30 mL of anhydrous toluene, followed by $Pd(dba)_3$ (0.044 g, 0.05 mmol), $P(^tBu)_3 \cdot HBF_4$ (0.032 g, 0.05 mmol) and solid Cs_2CO_3 (0.652 g, 2.0 mmol). The mixed solution was heated to 110°C under nitrogen protection and refluxed for 24 hours. The organic phase was extracted with methylene chloride and filtered by vacuum to obtain a crude product. Subsequently, white solid compound **1** (0.15 g) was obtained by column chromatography using pure petroleum ether. ^{1}H NMR (400 MHz, $CDCl_3$) δ 7.61 (t, J = 7.7 Hz, 2H), 7.51-7.46 (m, 1H), 7.42-7.38 (m, 2H), 7.02 (dd, J = 7.3, 1.8 Hz, 2H), 6.88-6.78 (m, 4H), 6.20 (dd, J = 7.9, 1.5 Hz, 2H).

Synthesis of compound 2: In a 100 mL round-bottom flask wrapped with aluminum foil, a solution of NBS (1.068 g, 6.0 mmol) in dichloromethane (18 mL) was added dropwise to a solution of compound 1 (0.275 g, 1.0 mmol) in dichloromethane (10 mL). The resulting mixture was stirred on a stirrer for 12 hours. After vacuum filtration, a crude product was obtained and further purified by column chromatography (petroleum ether:ethyl acetate = 15:1, v/v) to give a light pink solid compound **2** (0.18 g). ^{1}H NMR (400 MHz, $CDCl_3$) δ 8.09 (d, J = 2.3 Hz, 1H), 7.85 (d, J = 8.6 Hz, 1H), 7.49 (dd, J = 9.1, 2.3 Hz, 1H), 7.28 (s, 1H), 6.59 (d, J = 9.1 Hz, 1H).

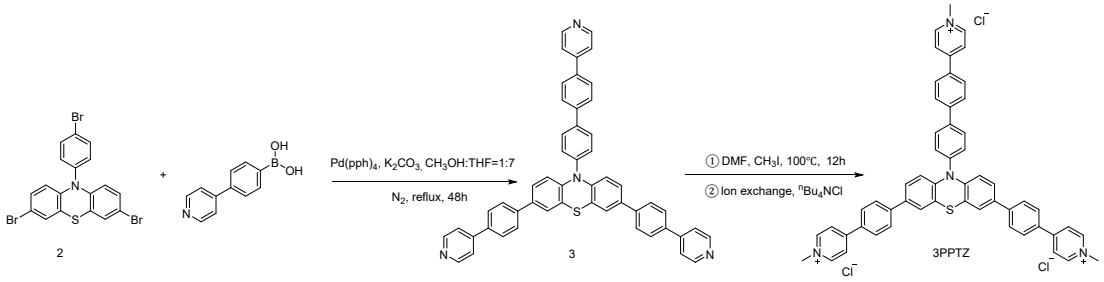

Scheme S2. Synthetic route of **compound 3** and **3PPTZ**.

Synthesis of compound 3: In a 100 mL round-bottom flask, (4-(pyridin-4-yl)phenyl)boronic acid (1.194 g, 6.0 mmol) was added to the mixed solution of compound **2** (0.512 g, 1.0 mmol) (toluene:THF=1:7, v/v), and then $Pd(pph_3)_4$ (0.115 g, 0.1 mmol)and 2 mol L^{-1} potassium carbonate aqueous solution (6.0 mL) were added sequentially. The mixed solution was refluxing at 110 ℃ for 48 h under nitrogen condition. The reaction solution is then cooled to room temperature and the solvent is evaporated under reduced pressure. The precipitate is dissolved in dichloromethane and washed three times with distilled water. After removing the solvent, the crude product was obtained, and then the target product compound **3** (0.16 g) was obtained by column chromatography (dichloromethane:methanol=50:1, v/v). ^{1}H NMR (400 MHz, $CDCl_3$) δ 8.72 (d, J = 6.0 Hz, 2H), 8.68 (d, J = 6.1 Hz, 4H), 8.32 (d, J = 2.2 Hz, 2H), 8.02 (d, J = 8.4 Hz, 2H), 7.85 (q, J = 8.5 Hz, 4H), 7.75 (s, 10H), 7.62-7.54 (m, 8H), 6.95 (d, J = 8.9 Hz, 2H).

Synthesis of 3PPTZ: Compound **3** (0.16 g) was dissolved in 5.0 mL of DMF and then 1.0 mL of CH_3I was added. The mixture was then refluxed for 12 hours. After cooling to room temperature, it was washed with ethyl acetate and filtered to obtain a reddish-brown product. After further purification by ion exchange, the final target compound **3PPTZ** (0.12 g), was obtained. ^{1}H NMR (400 MHz, DMSO-d_6) δ 8.99 (d, J = 7.0 Hz, 6H), 8.58 (dd, J = 30.7, 7.0 Hz, 6H), 8.28 (d, J = 8.6 Hz, 2H), 8.21 - 8.11 (m, 8H), 7.91 (d, J = 8.6 Hz, 4H), 7.70 (s, 2H), 7.64 (d, J = 2.2 Hz, 2H), 7.47 (d, J = 10.8 Hz, 2H), 6.33 (d, J = 8.6 Hz, 2H), 4.34 (d, J = 13.7 Hz, 9H).

2 Experimental data

2.1 ^{1}H NMR data of compound

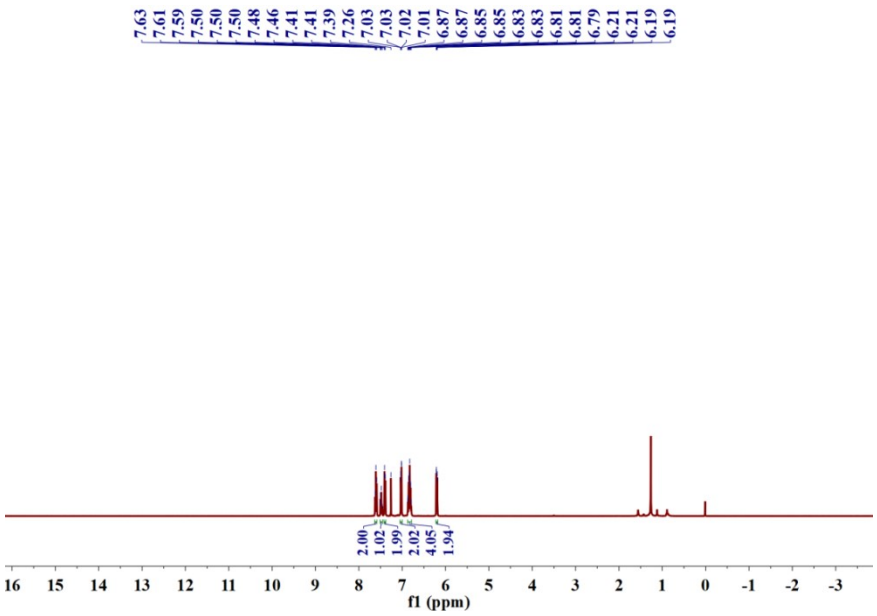

Fig. S1. ^{1}H NMR spectrum of compound **1** in $CDCl_3$.

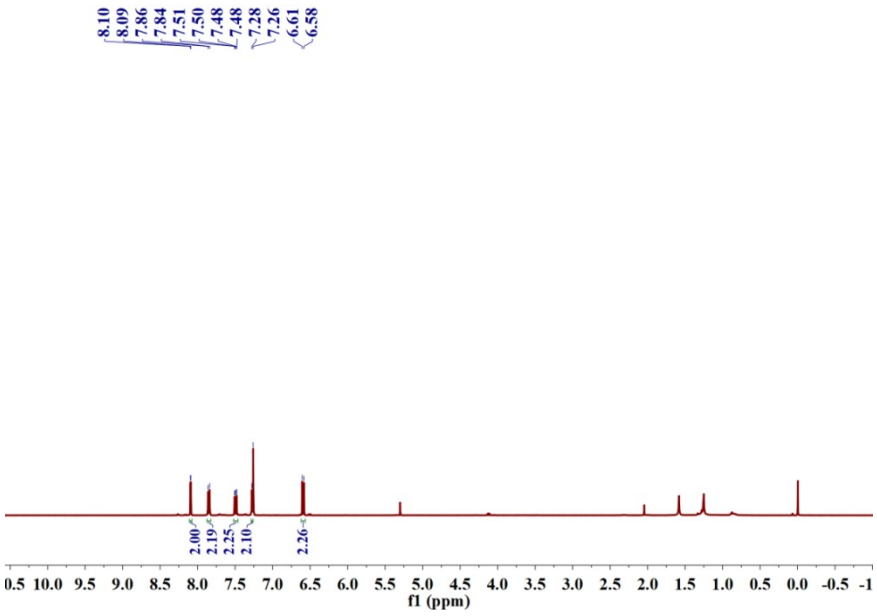

Fig. S2. ^{1}H NMR spectrum of compound **2** in $CDCl_3$.

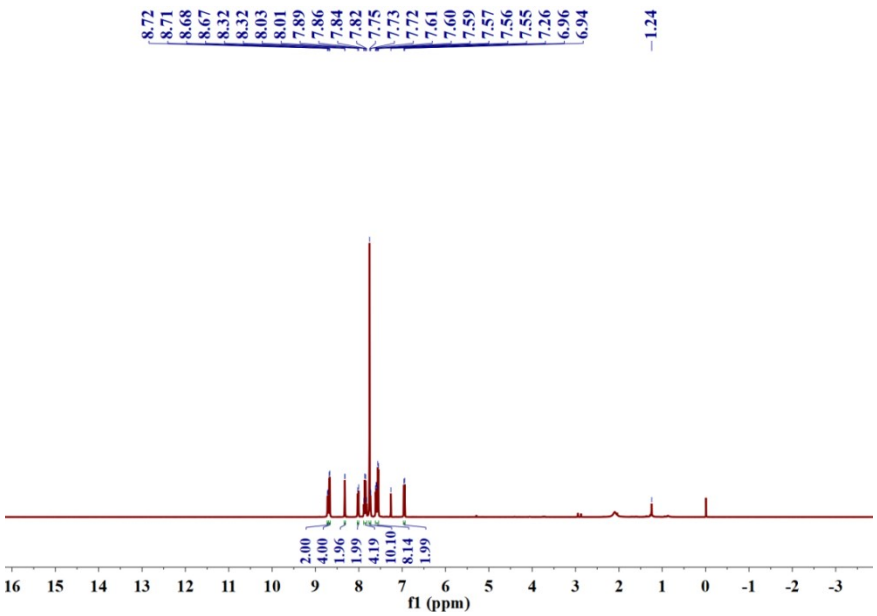

Fig. S3. ^{1}H NMR spectrum of compound **3** in $CDCl_3$.

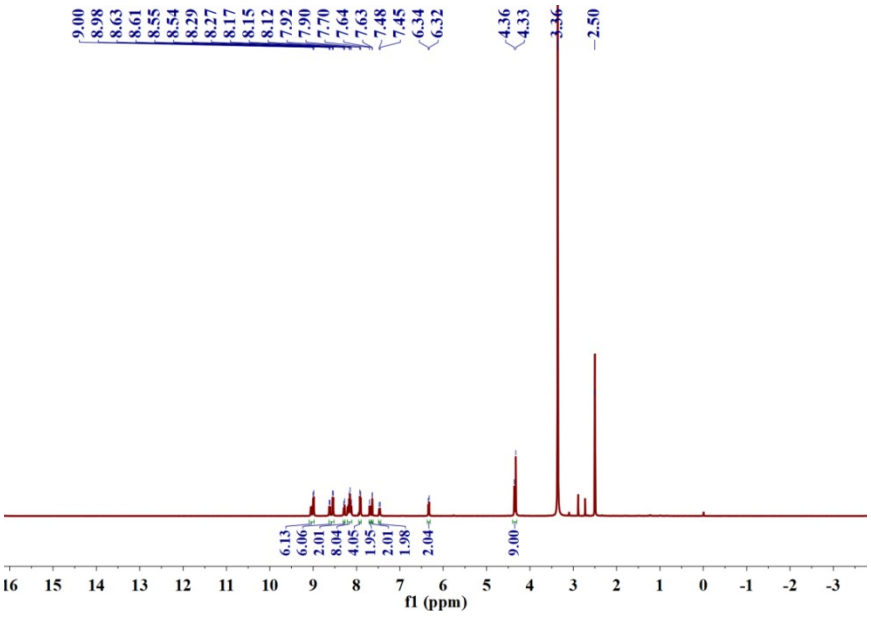

Fig. S4. ^{1}H NMR spectrum of compound **3PPTZ** in DMSO-d_6

2.2 Fluorescence quantum yields

Table S1. Fluorescence quantum yields of 3PPTZ and 3PPTZ-CB[8].

Entry	Systems	Quantum Yieldb[%]
1	3PPTZ	1.7
2	3PPTZ-CB[8]	0.5

2.3 ^{1}H NMR titration experiments

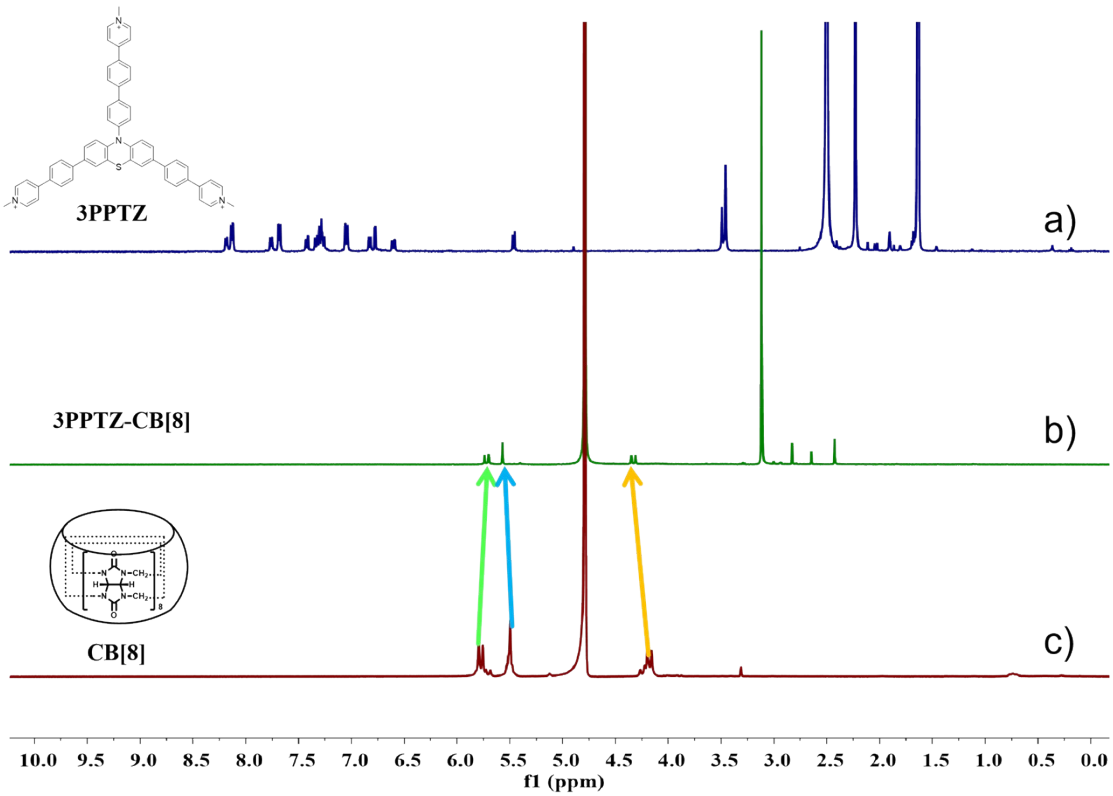

Fig. S5. ^{1}H NMR spectra of a) 3PPTZ (5×10^{-4} mol/L) in DMSO-d_6 (0.5 mL), b) 3PPTZ-CB[8] (5×10^{-4} mol/L) and c) CB[8] (5×10^{-4} mol/L) in D_2O (0.5 mL).

2.4 Dynamic light scattering

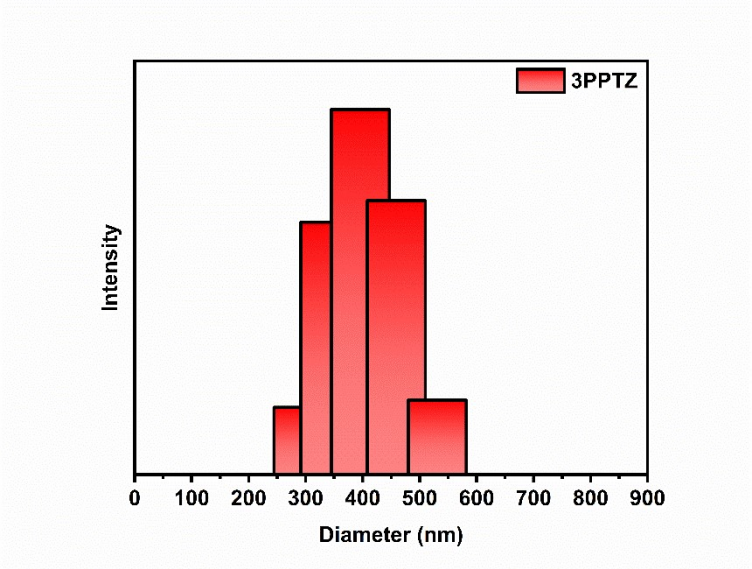

Fig. S6 DLS result of 3PPTZ.

2.5 $^1O_2$ detection experiment

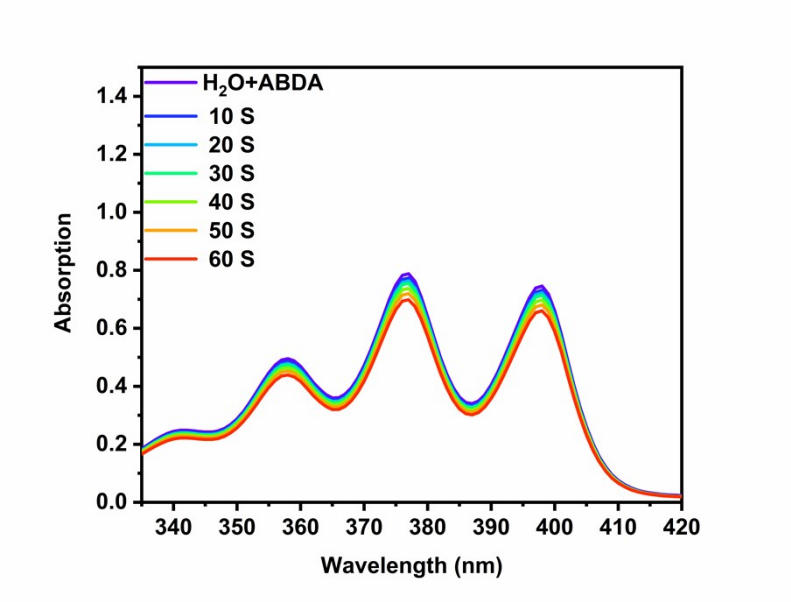

Fig. S7. The absorption spectra of ABDA after irradiation (430-440 nm, 18 W) for different time in the presence of H_2O (3 mL).

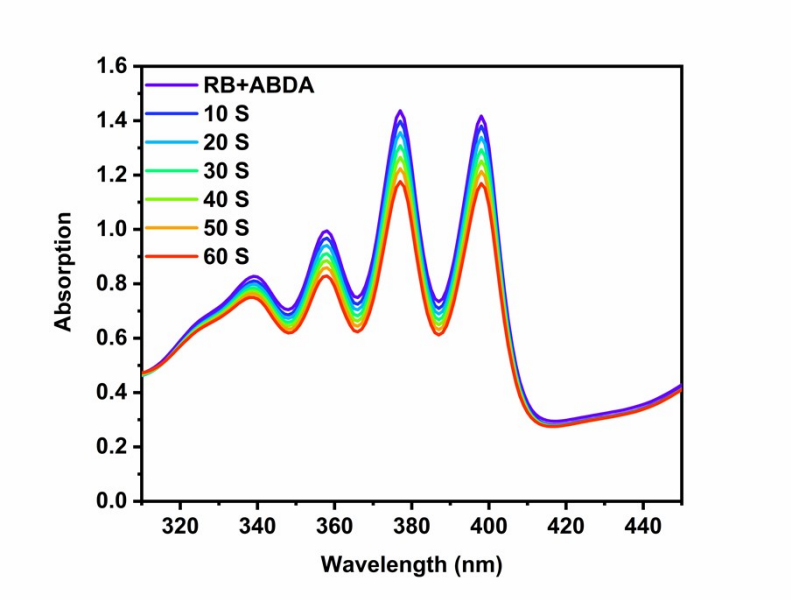

Fig. S8. The absorption spectra of ABDA after irradiation (430-440 nm, 18 W) for different time in the presence of RB (2.0×10^{-5} mol/L) aqueous solution.

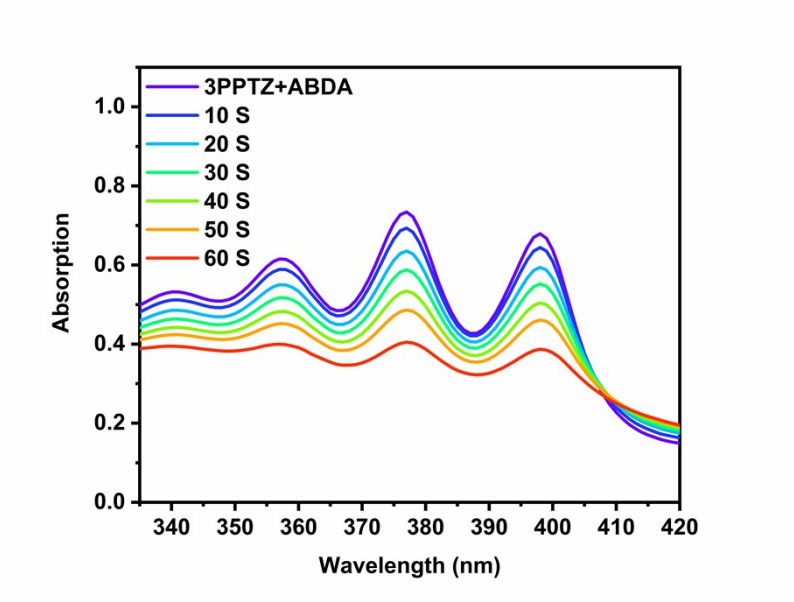

Fig. S9. The absorption spectra of ABDA after irradiation (430-440 nm, 18 W) for different times in the presence of 3PPTZ (2.0×10^{-5} mol/L) aqueous solution.

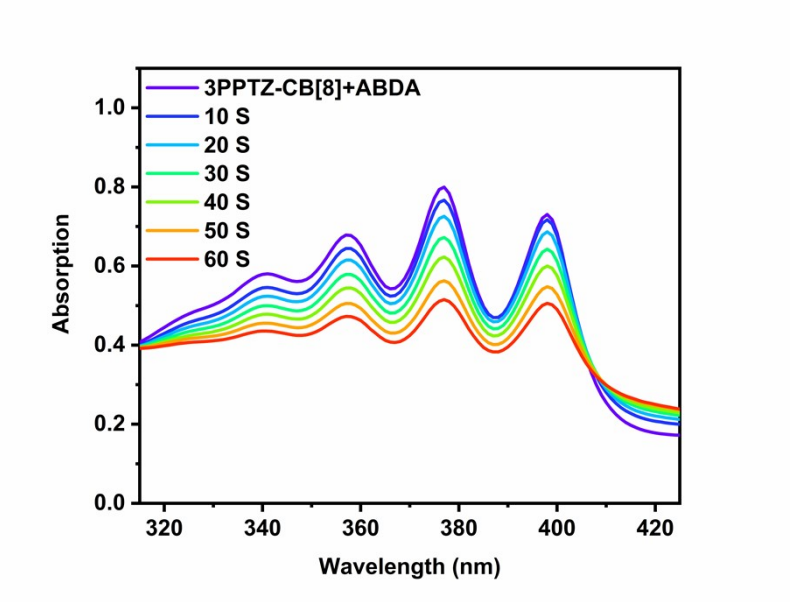

Fig. S10. The absorption spectra of ABDA after irradiation (430-440 nm, 18 W) for different time in the presence of 3PPTZ-CB[8] (2.0×10^{-5} mol/L) aqueous solution.

2.6 Schematic diagram of the mechanism of $^1O_2$ and $O_2^{\bullet-}$

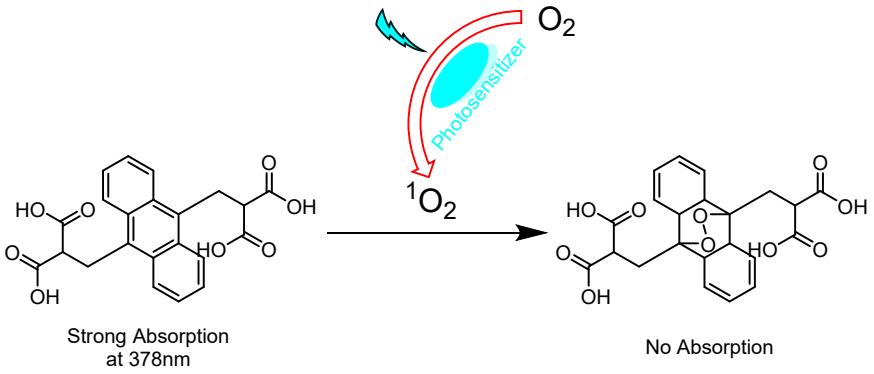

Fig. S11. Schematic diagram of the mechanism by which ABDA interact with oxygen to generate singlet oxygen ($^1O_2$) . Compound 9,10-anthracenediyl-bis(methylene)-dimalonic acid (ABDA) was used as an indicator for detection of $^1O_2$ in solution. 40 μM of photocatalyst was dissolved in 3 mL solution containing 0.1 mM of ABDA. The mixture was then placed in a cuvette and irradiated with a blue light (430-440 nm). The absorption change of the sample at 378 nm was recorded by the UV-Vis absorption spectrophotometer. $^1O_2$ is generated through the Type II photosensitizer pathway: the ground state oxygen ($^3O_2$) receives energy from the triplet photosensitizer and transitions to the excited state, converting to $^1O_2$. As a specific probe for $^1O_2$, ABDA undergoes a [4+2] cycloaddition reaction with $^1O_2$ to form an internal peroxide, accompanied by a decrease in the characteristic absorbance at 400 nm, thereby achieving qualitative and quantitative detection of $^1O_2$.

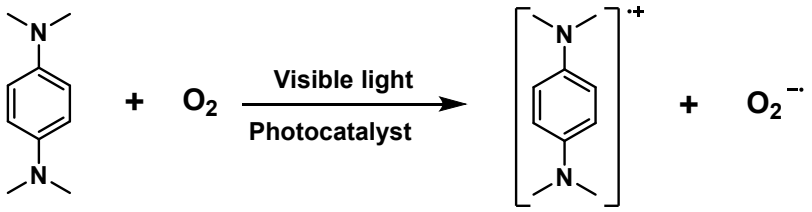

Fig. S12. Schematic diagram of the mechanism by which TMPD interact with oxygen to superoxide anion radicals ($O_2^{\bullet-}$). N, N, N', N'-tetramethyl-phenylenediamine (TMPD) was used as the scavenger monitors $O_2^{\bullet-}$. The 5 mM TMPD solution in DMSO was added to the aqueous solution to form a 0.1 mM solution. 40 μM photocatalyst were added into TMPD solution respectively for $O_2^{\bullet-}$ generation measurement. The mixture was then placed in a cuvette and irradiated with a blue light (430-440 nm). The generation of $O_2^{\bullet-}$ was detected by monitoring the absorption at 612 nm through UV-vis absorption spectra. The triplet excited state photosensitizer ($^3PS^*$) has strong oxidative activity and can take a single electron from the TMPD molecule to undergo redox reactions, generating photosensitizer anionic radicals ($PS^{-\bullet}$) and TMPD cationic radicals ($TMPD^{+\bullet}$); $PS^{-\bullet}$ Immediately transfers a single electron to $^3O_2$, completing the regeneration of the ground state photosensitizer, while reducing $^3O_2$ to $O_2^{\bullet-}$.

2.7 Procedure for $^1O_2$ quantum yield measurement

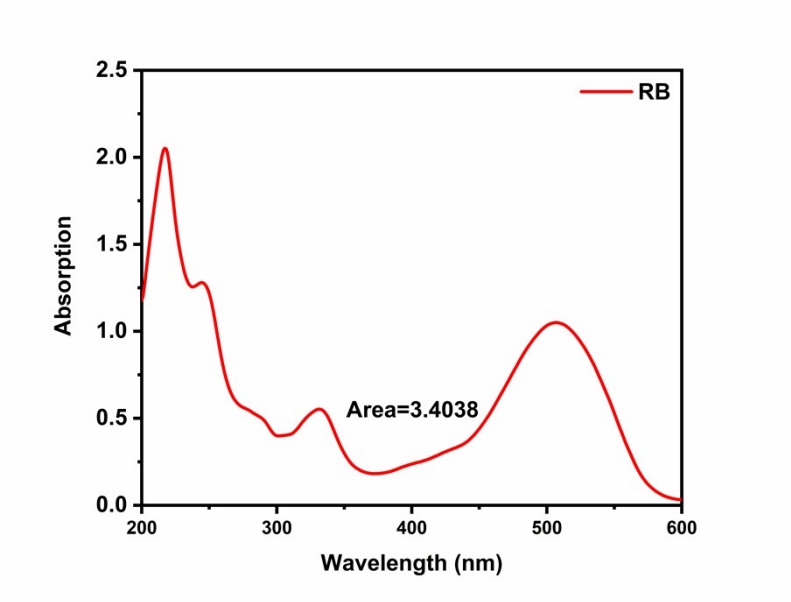

Fig. S13. The UV-vis absorption spectra of RB (2.0×10^{-5} mol/L) in the aqueous solution.

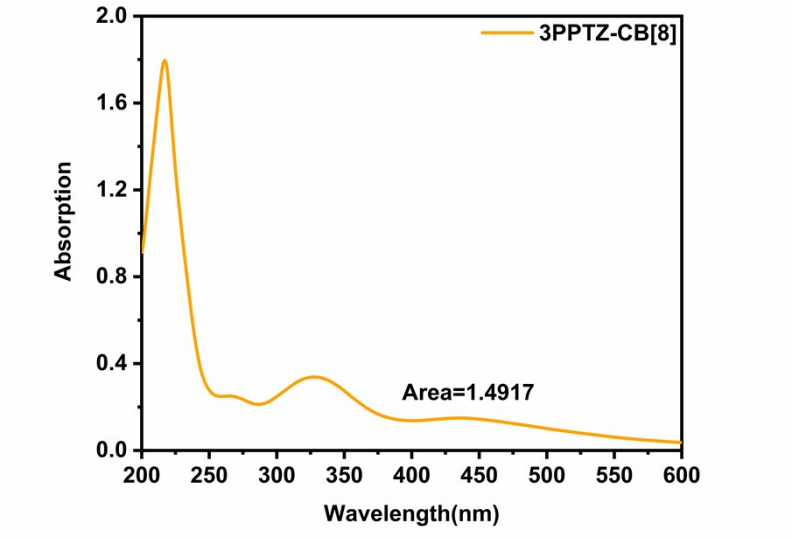

Fig. S14. The UV-vis absorption spectra of 3PPTZ (2.0×10^{-5} mol/L) in the aqueous solution.

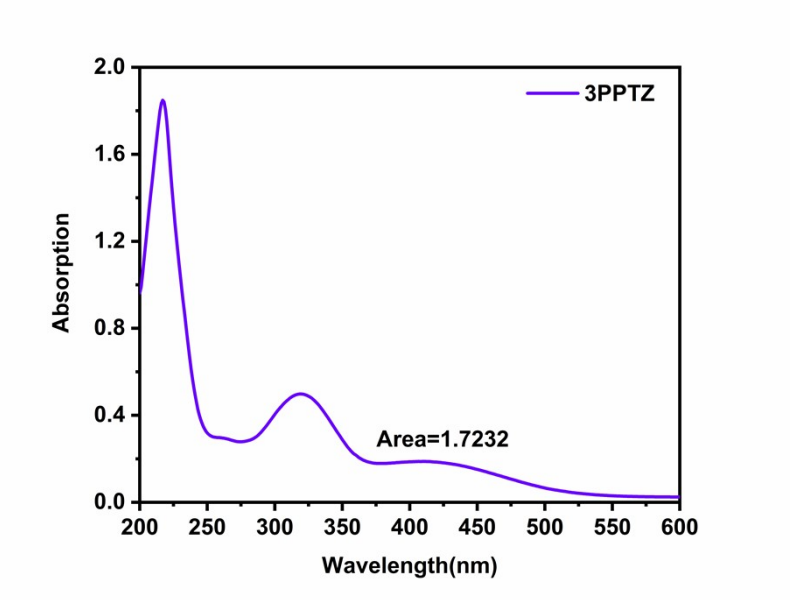

Fig. S15. The UV-vis absorption spectra of 3PPTZ-CB[8] (2.0×10^{-5} mol/L) in the aqueous solution.

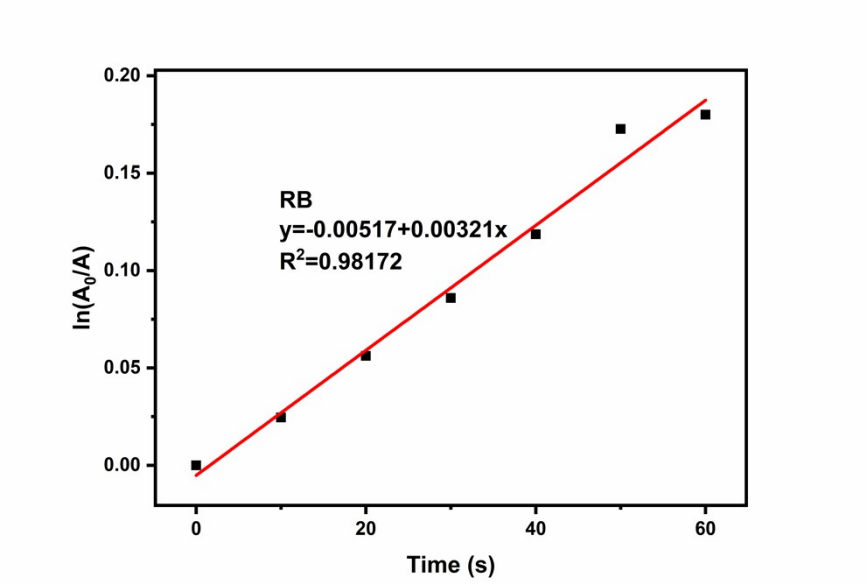

Fig. S16. The UV-vis absorption spectra of RB (2.0×10^{-5} mol/L) in the aqueous solution.

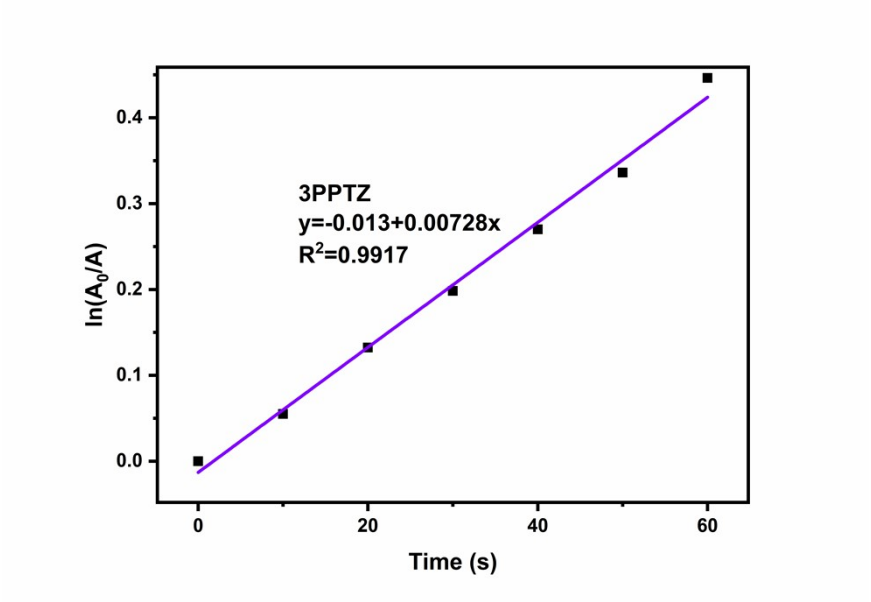

Fig. S17. The UV-vis absorption spectra of 3PPTZ (2.0×10^{-5} mol/L) in the aqueous solution.

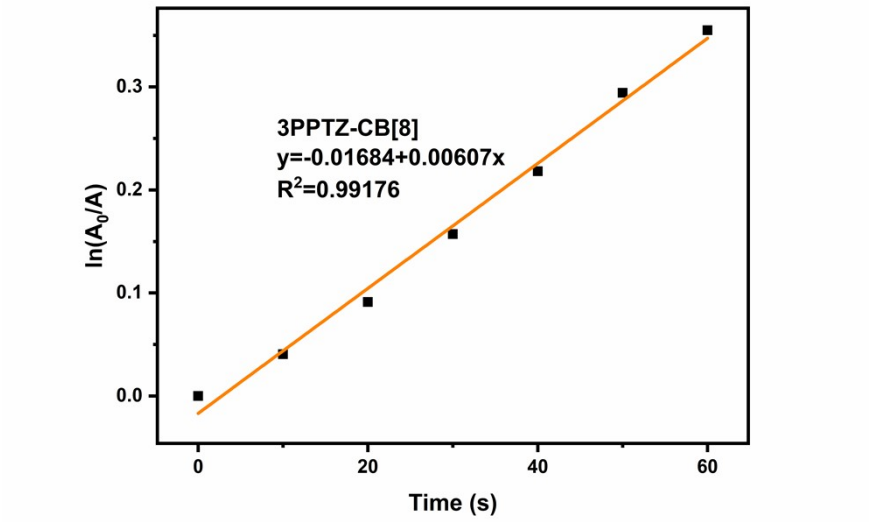

Fig. S18. The UV-vis absorption spectra of 3PPTZ-CB[8] (2.0×10^{-5} mol/L) in the aqueous solution.

2.8 Electron paramagnetic resonance

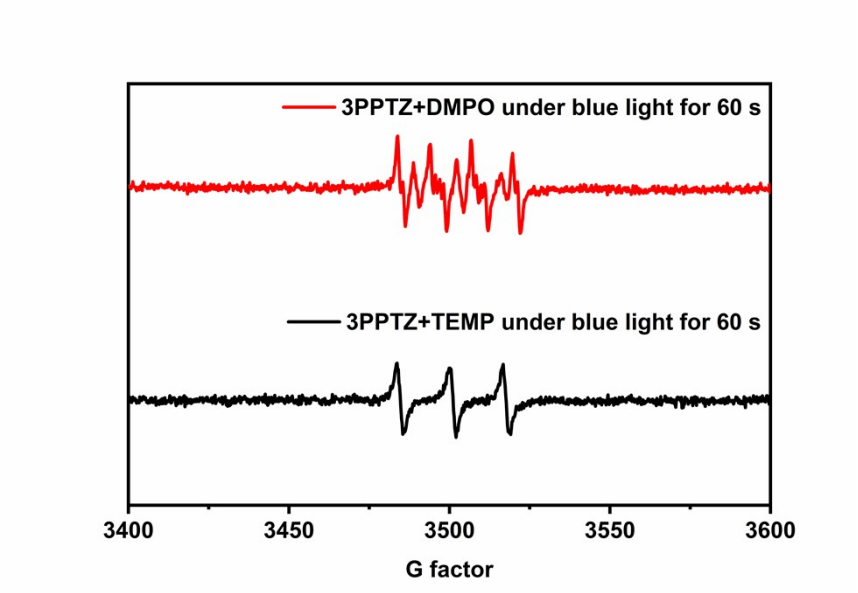

Fig. S19. EPR spectra for capturing $^1O_2$ with TEMP serving as the trapping agent in aqueous solution and EPR spectra for capturing $O_2^{\bullet-}$ with DMPO serving as the trapping agent in aqueous solution.

2.9 Fluorescence emission spectra

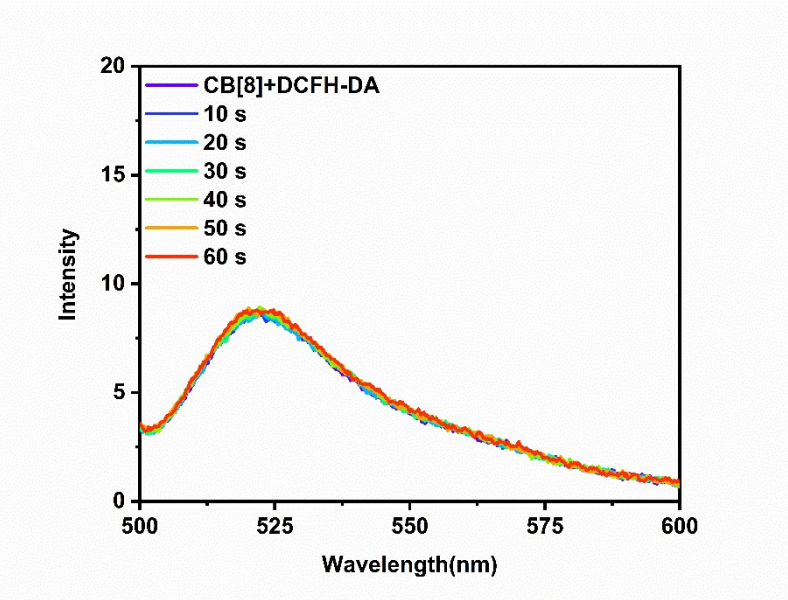

Fig. S20. Fluorescence emission spectra of CB[8] in the presence of DCFH under the purple light irradiation.

2.10 Gram scale reaction for photocatalytic synthesis of benzothiazole

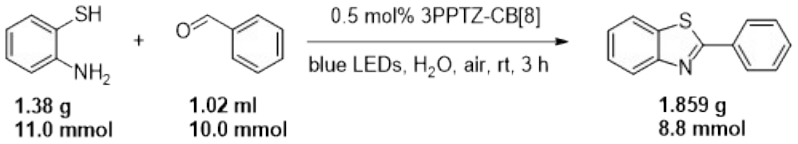

For this reaction, benzaldehyde (1.02 mL, 10.0 mmol) and 2-aminothiophenol (1.38 g, 11.0 mmol) were dissolved in water (30 mL) in a 50 mL Pyrex tube. Then 3PPTZ-CB[8] (0.5 mol%) was added to the above solution. The reaction mixture is magnetically stirred at 1500 rpm and irradiated with blue light (18 W) in an open system. An electric fan is added to ensure the reaction proceeds at room temperature for 3 hours. Afterwards, the mixture is extracted with ethyl acetate, the organic layers are combined, and dried over anhydrous sodium sulfate. The organic solvent is then concentrated under vacuum. The crude product is purified by quick column chromatography using petroleum ether/ethyl acetate to afford the product in 88% yield (1.86 g, 8.8 mmol).

2.11 Detection of hydrogen peroxide

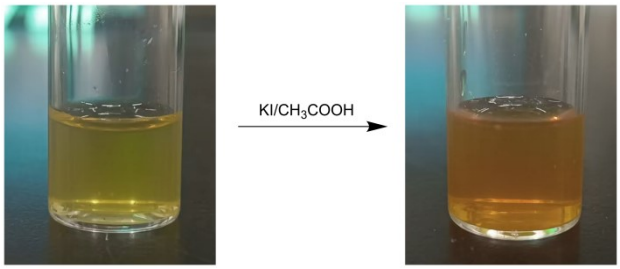

Fig. S21. Detection of hydrogen peroxide in the photocatalytic synthesis of 2-phenylbenzothiazole with KI/CH_3COOH. To water (3 mL) were added 2-aminobenzenethiol (0.22 mmol), benzaldehyde (0.2 mmol), and the catalyst 3PPTZ-CB[8] (0.5 mol%). After irradiation under an air atmosphere for 3 hours, the aqueous layer was collected, and 0.1 M aqueous KI solution and 0.1 M aqueous acetic acid solution were added to the filtrate, resulting in a color change of the reaction mixture from yellow to brown, and confirming the generation of hydrogen peroxide in the proposed reaction pathway.

3 ^{1}H NMR data of 3a-3y

3a. 2-phenylbenzo[d]thiazole (93% yield)

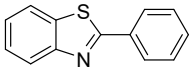

^{1}H NMR (400 MHz, $CDCl_3$) δ 8.10 (dd, J = 3.9, 2.3 Hz, 3H), 7.91 (dd, J = 8.0, 1.1 Hz, 1H), 7.50 (t, J = 3.2 Hz, 4H), 7.42 - 7.37 (m, 1H).

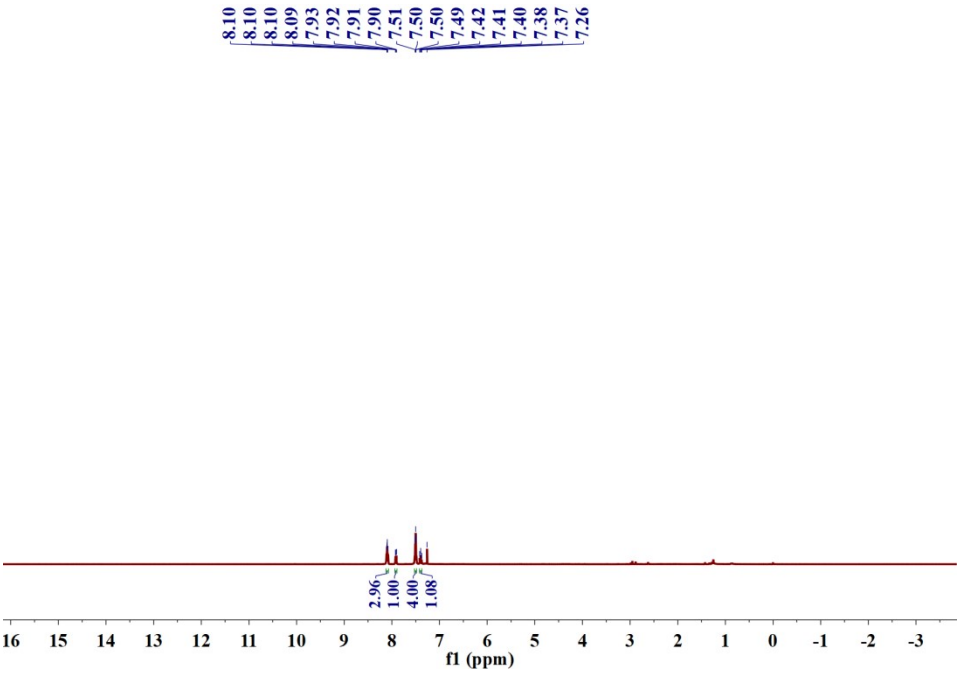

Fig. S22. ^{1}H NMR spectra of 2-phenylbenzo[d]thiazole in $CDCl_3$.

3b. 2-(o-tolyl)benzo[d]thiazole (86% yield)

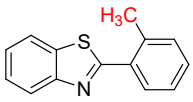

^{1}H NMR (400 MHz, $CDCl_3$) δ 8.11 (d, J = 8.2 Hz, 1H), 7.94 (d, J = 7.4 Hz, 1H), 7.76 (d, J = 7.4 Hz, 1H), 7.54-7.49 (m, 1H), 7.44 - 7.29 (m, 4H), 2.66 (s, 3H).

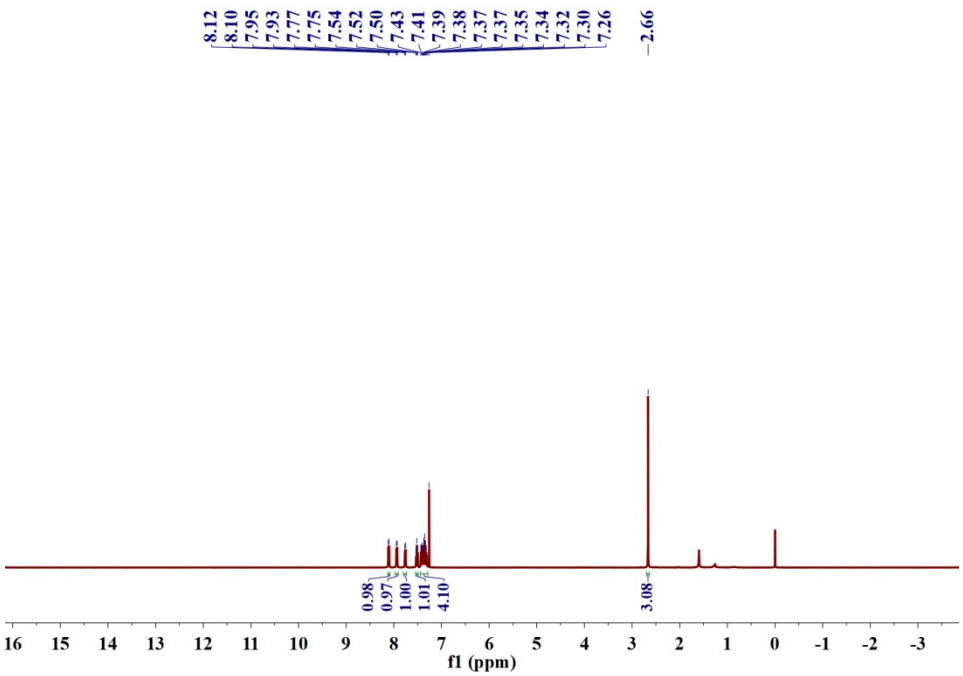

Fig. S23. ^{1}H NMR spectra of 2-(o-tolyl)benzo[d]thiazole in $CDCl_3$.

3c. 2-(3,5-dimethylphenyl)benzo[d]thiazole (91% yield)

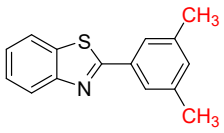

^{1}H NMR (400 MHz, $CDCl_3$) δ 8.08 (d, J = 8.1 Hz, 1H), 7.90 (d, J = 8.4 Hz, 1H), 7.72 (s, 2H), 7.49 (t, J = 8.3 Hz, 1H), 7.38 (t, J = 7.6 Hz, 1H), 7.13 (s, 1H), 2.41 (s, 6H).

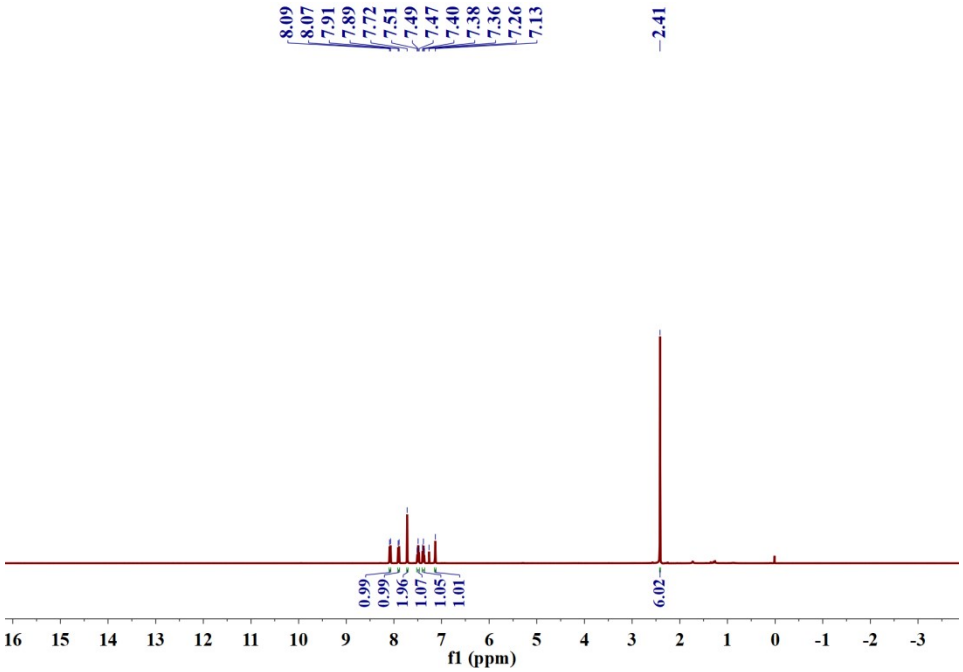

Fig. S24. ^{1}H NMR spectra of 2-(3,5-dimethylphenyl)benzo[d]thiazole in $CDCl_3$.

3d. 2-(p-tolyl)benzo[d]thiazole (95% yield)

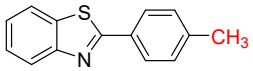

^{1}H NMR (400 MHz, $CDCl_3$) δ 8.06 (d, J = 8.1 Hz, 1H), 7.99 (d, J = 8.2 Hz, 2H), 7.90 (d, J = 8.0 Hz, 1H), 7.49 (t, J = 7.1 Hz, 1H), 7.38 (t, J = 8.1 Hz, 1H), 7.31 (d, J = 7.9 Hz, 2H), 2.43 (s, 3H).

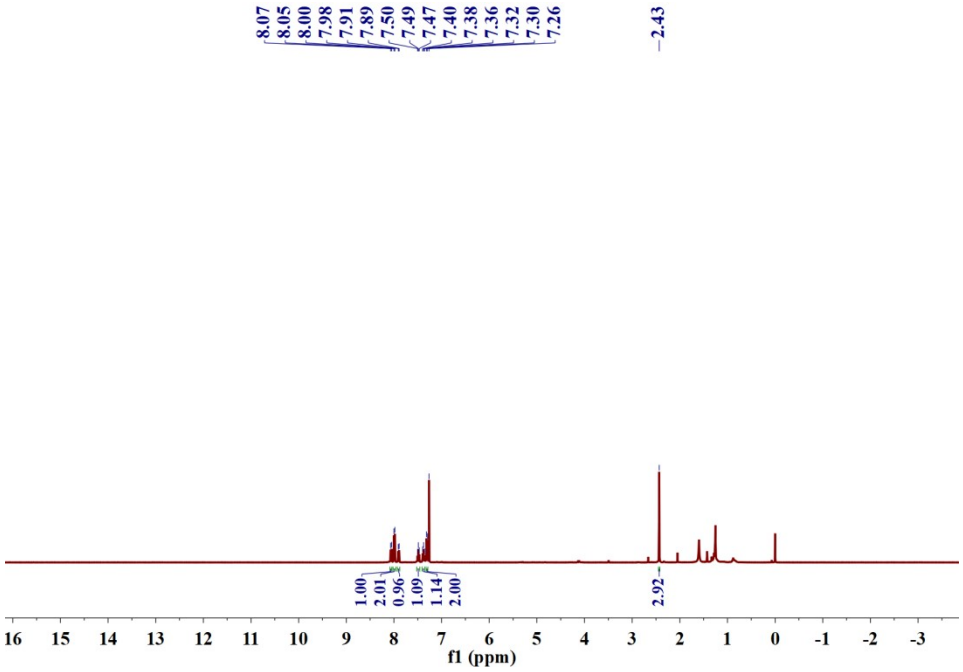

Fig. S25. ^{1}H NMR spectra of 2-(p-tolyl)benzo[d]thiazole in $CDCl_3$.

3e. 2-(2,5-dimethoxyphenyl)benzo[d]thiazole (84% yield)

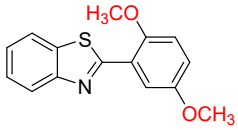

^{1}H NMR (400 MHz, DMSO-d_6) δ 8.14 (d, J = 7.9 Hz, 1H), 8.09 (d, J = 7.9 Hz, 1H), 7.98 (d, J = 3.2 Hz, 1H), 7.58 - 7.52 (m, 1H), 7.48 - 7.42 (m, 1H), 7.26 (d, J = 9.1 Hz, 1H), 7.16 (dd, J = 9.1, 3.2 Hz, 1H), 4.02 (s, 3H), 3.84 (s, 3H).

.

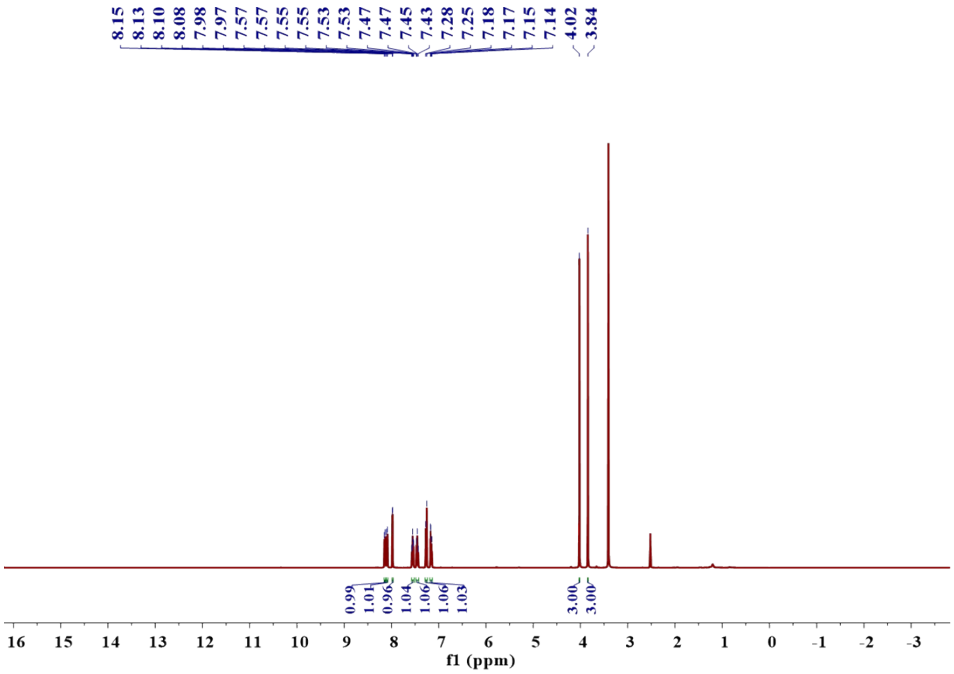

Fig. S26. ^{1}H NMR spectra of 2-(2,5-dimethoxyphenyl)benzo[d]thiazole in DMSO-d_6.

3f. 4-(benzo[d]thiazol-2-yl)-3-methoxy-N,N-dimethylaniline (72% yield)

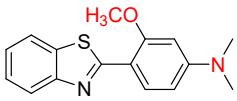

^{1}H NMR (400 MHz, DMSO-d_6) δ 8.24 (d, J = 8.9 Hz, 1H), 8.02 (d, J = 7.6 Hz, 1H), 7.92 (d, J = 8.0 Hz, 1H), 7.48 - 7.43 (m, 1H), 7.32 (t, J = 8.0 Hz, 1H), 6.50 (dd, J = 9.0, 2.3 Hz, 1H), 6.38 (d, J = 2.3 Hz, 1H), 4.04 (s, 3H), 3.05 (s, 6H).

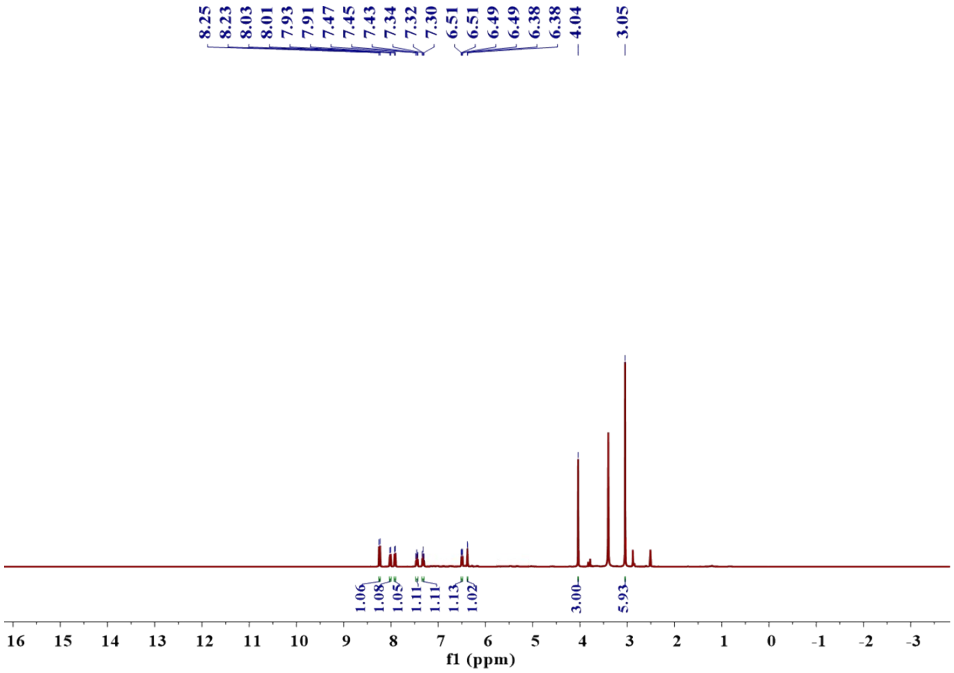

Fig. S27. ^{1}H NMR spectra of 4-(benzo[d]thiazol-2-yl)-3-methoxy-N,N-dimethyla niline in DMSO-d_6.

3g. 2-(2-fluorophenyl)benzo[d]thiazole (73% yield)

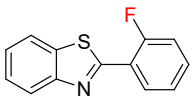

^{1}H NMR (400 MHz, $CDCl_3$) δ 8.43 (td, J = 7.7, 1.8 Hz, 1H), 8.13 (d, J = 8.2 Hz, 1H), 7.95 (d, J = 7.9 Hz, 1H), 7.55 - 7.39 (m, 3H), 7.32 (t, J = 7.6 Hz, 1H), 7.28 - 7.21 (m, 1H).

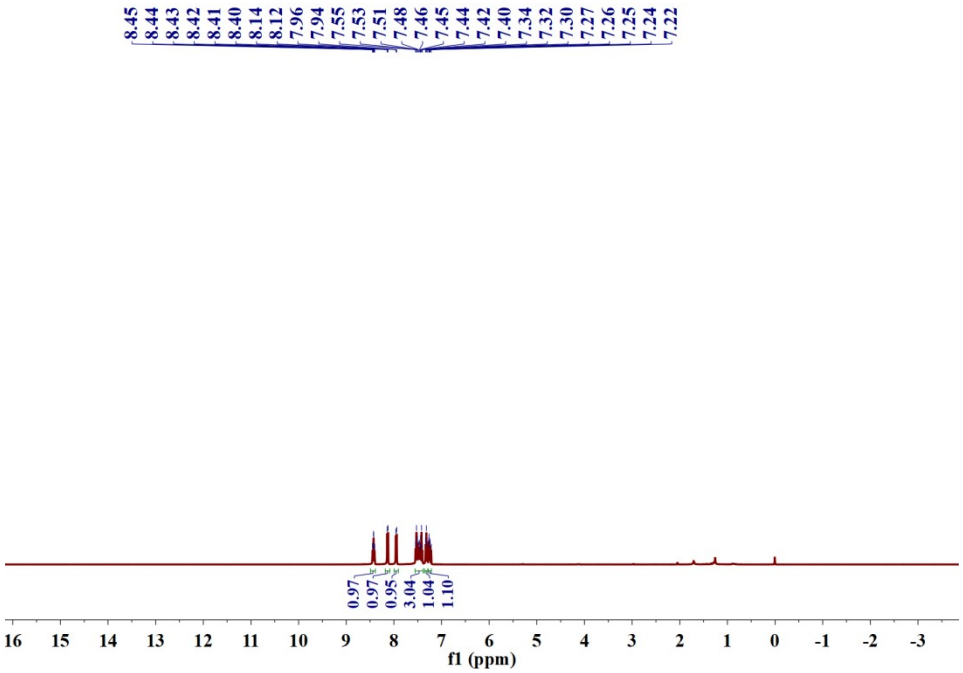

Fig. S28. ^{1}H NMR spectra of 2-(2-fluorophenyl)benzo[d]thiazole in $CDCl_3$.

3h. 2-(3,5-difluorophenyl)benzo[d]thiazole (91% yield)

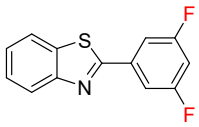

^{1}H NMR (400 MHz, $CDCl_3$) δ 8.09 (d, J = 8.5 Hz, 1H), 7.92 (d, J = 8.0 Hz, 1H), 7.62 (dd, J = 8.0, 2.2 Hz, 2H), 7.53 (td, J = 8.3, 7.8, 1.2 Hz, 1H), 7.45 - 7.41 (m, 1H), 6.93 (tt, J = 8.6, 2.3 Hz, 1H).

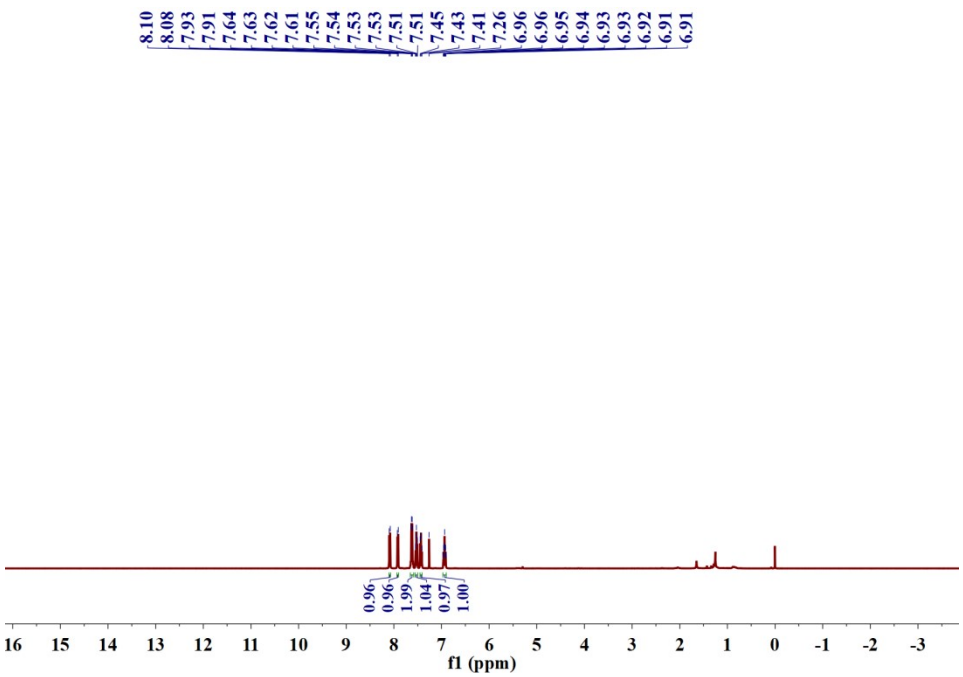

Fig. S29. ^{1}H NMR spectra of 2-(3,5-difluorophenyl)benzo[d]thiazole in $CDCl_3$.

3i. 2-(4-fluorophenyl)benzo[d]thiazole (84% yield)

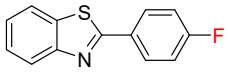

^{1}H NMR (400 MHz, $CDCl_3$) δ 8.13-8.02 (m, 3H), 7.91 (d, J = 8.0 Hz, 1H), 7.54-7.47 (m, 1H), 7.40 (t, J = 8.2 Hz, 1H), 7.19 (t, J = 8.6 Hz, 2H).

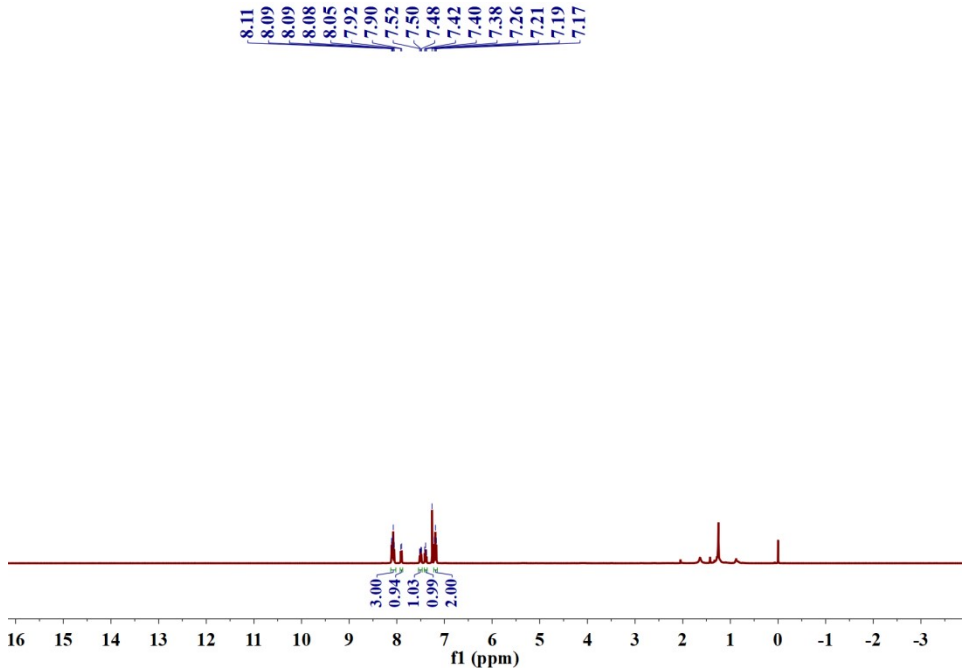

Fig. S30. ^{1}H NMR spectra of 2-(4-fluorophenyl)benzo[d]thiazole in $CDCl_3$.

3j. 2-(4-chlorophenyl)benzo[d]thiazole (89% yield)

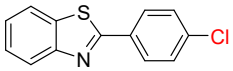

^{1}H NMR (400 MHz, $CDCl_3$) δ 8.42 (td, J = 7.7, 1.8 Hz, 1H), 8.13 (d, J = 8.2 Hz, 1H), 7.95 (d, J = 7.9 Hz, 1H), 7.54 - 7.39 (m, 3H), 7.31 (t, J = 8.1 Hz, 1H), 7.27 - 7.21 (m, 1H).

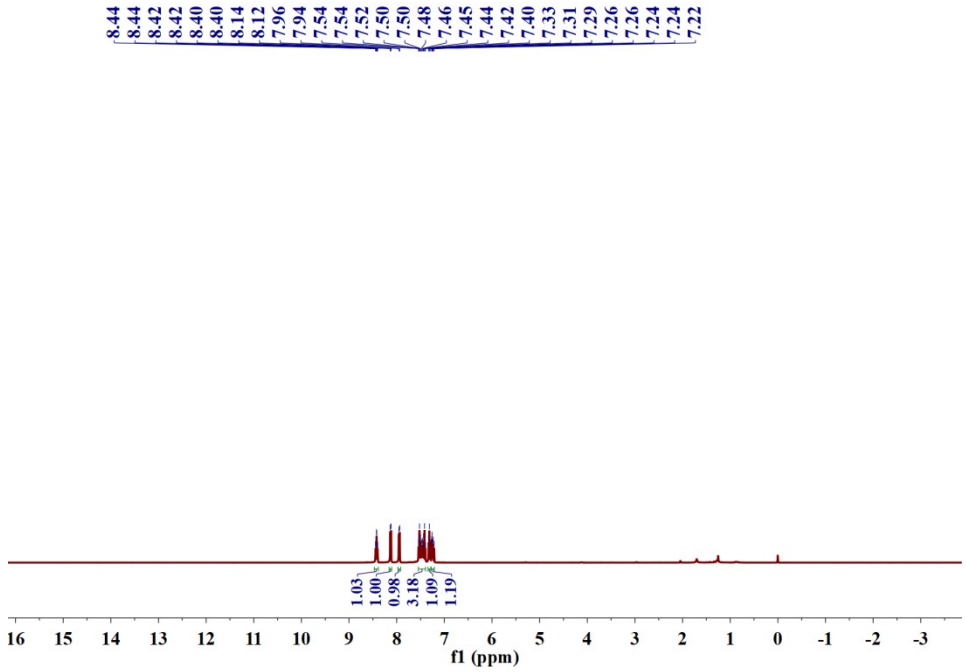

Fig. S31. ^{1}H NMR spectra of 2-(4-chlorophenyl)benzo[d]thiazole in $CDCl_3$.

3k. 2-(2-chlorophenyl)benzo[d]thiazole (79% yield)

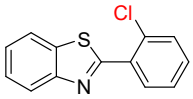

^{1}H NMR (400 MHz, $CDCl_3$) δ 8.22 (dd, J = 6.2, 3.4 Hz, 1H), 8.14 (d, J = 8.1 Hz, 1H), 7.96 (d, J = 7.9 Hz, 1H), 7.57 - 7.50 (m, 2H), 7.47 - 7.39 (m, 3H).

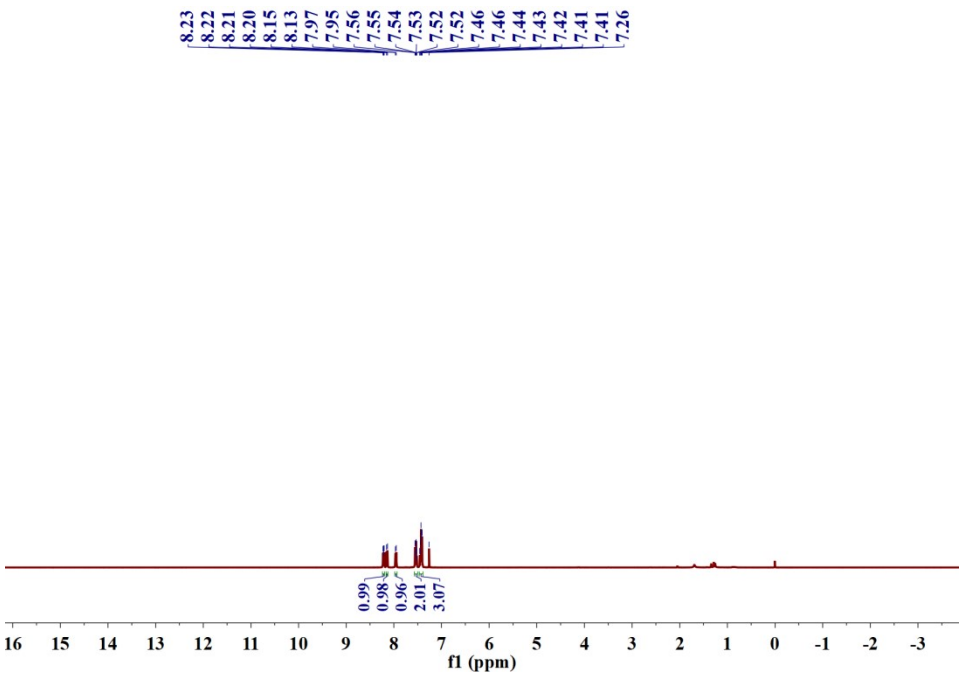

Fig. S32. ^{1}H NMR spectra of 2-(2-chlorophenyl)benzo[d]thiazole in $CDCl_3$.

3l. 2-(4-fluorophenyl)benzo[d]thiazole (92% yield)

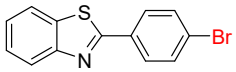

^{1}H NMR (400 MHz, $CDCl_3$) δ 8.07 (d, J = 8.4 Hz, 1H), 7.96 (d, J = 8.5 Hz, 2H), 7.91 (d, J = 8.0 Hz, 1H), 7.63 (d, J = 8.5 Hz, 2H), 7.51 (t, J = 8.1 Hz, 1H), 7.40 (t, J = 7.6 Hz, 1H).

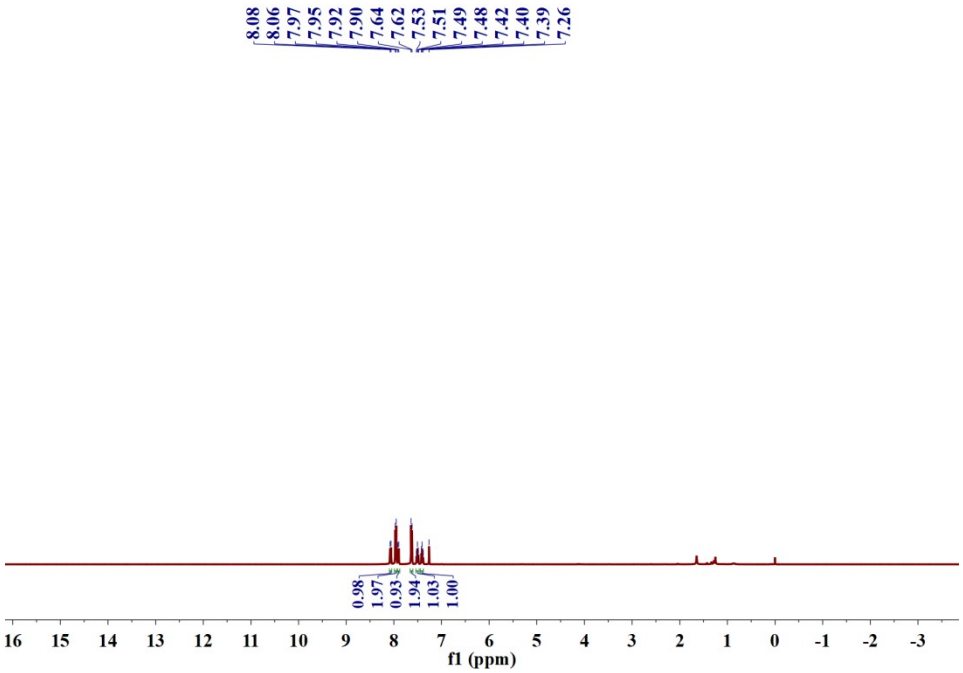

Fig. S33. ^{1}H NMR spectra of 2-(4-fluorophenyl)benzo[d]thiazole in $CDCl_3$.

3m. 2-(4-nitrophenyl)benzo[d]thiazole (88% yield)

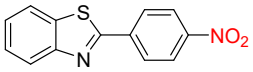

^{1}H NMR (400 MHz, $CDCl_3$) δ 8.36 (d, J = 8.9 Hz, 2H), 8.28 (d, J = 8.9 Hz, 2H), 8.14 (d, J = 8.0 Hz, 1H), 7.97 (d, J = 8.0 Hz, 1H), 7.59 - 7.54 (m, 1H), 7.47 (t, J = 8.2 Hz, 1H).

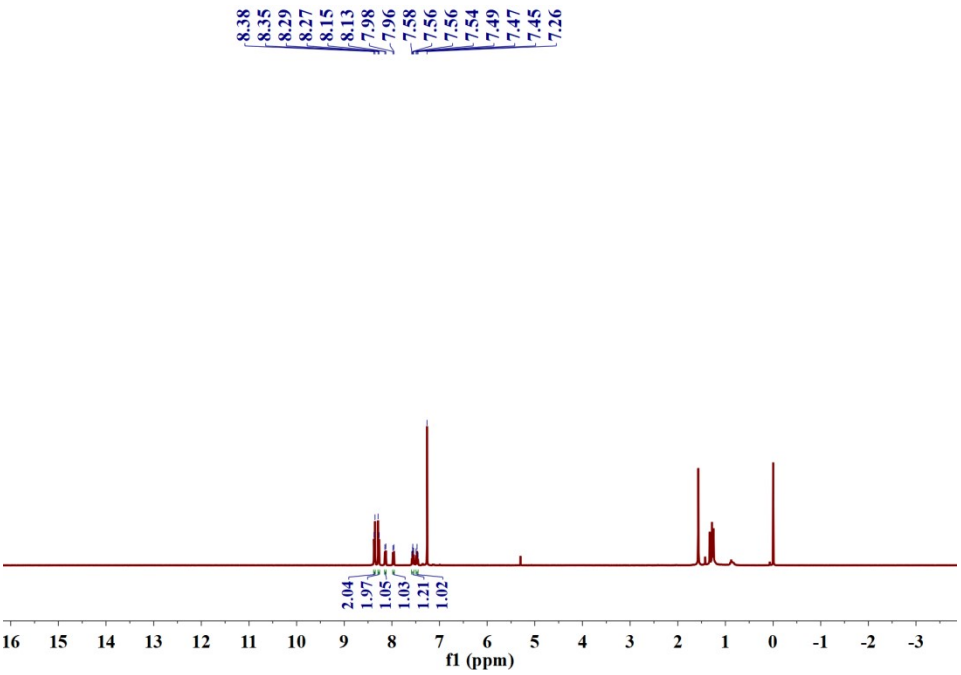

Fig. S34. ^{1}H NMR spectra of 2-(4-nitrophenyl)benzo[d]thiazole in $CDCl_3$.

3n. 5-chloro-2-phenylbenzo[d]thiazole (86% yield)

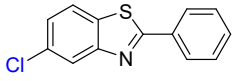

^{1}H NMR (400 MHz, $CDCl_3$) δ 8.12-8.04 (m, 3H), 7.82 (d, J = 8.5 Hz, 1H), 7.51 (d, J = 6.9 Hz, 3H), 7.37 (dd, J = 8.5, 2.0 Hz, 1H).

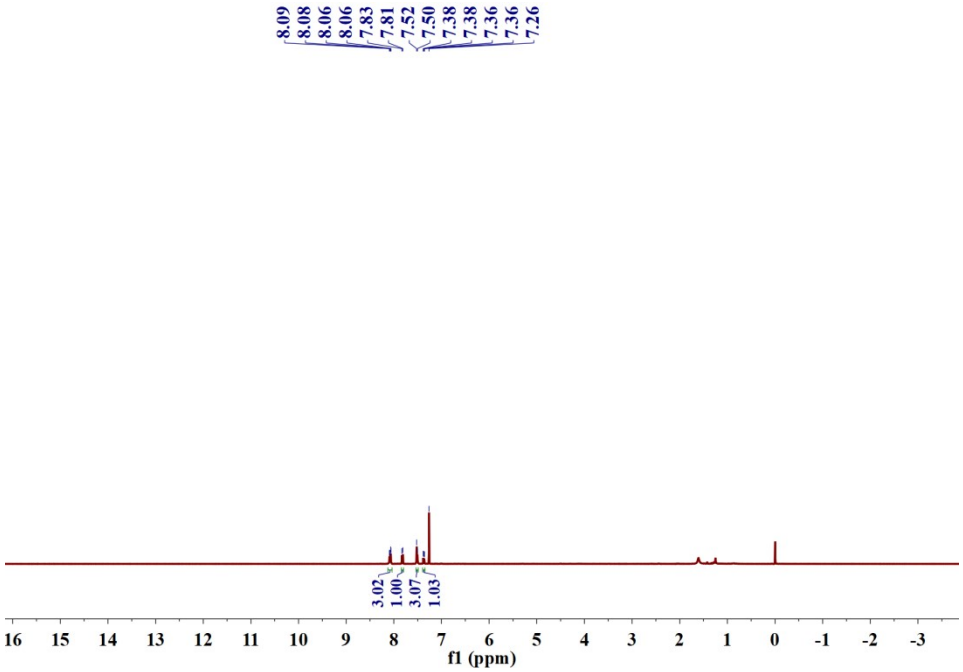

Fig. S35. ^{1}H NMR spectra of 5-chloro-2-phenylbenzo[d]thiazole in $CDCl_3$.

3o. 4-(5-chlorobenzo[d]thiazol-2-yl)-N,N-diphenylaniline (66% yield)

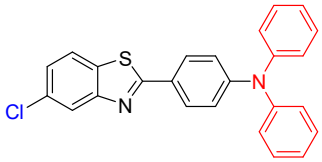

^{1}H NMR (400 MHz, DMSO-d_6) δ 8.14 (d, J = 8.6 Hz, 1H), 8.06 (d, J = 2.0 Hz, 1H), 7.95 (d, J = 8.9 Hz, 2H), 7.48 - 7.44 (m, 1H), 7.42 (s, 1H), 7.38 (s, 1H), 7.21 - 7.15 (m, 6H), 7.01 (s, 1H), 6.99 (s, 1H).

.

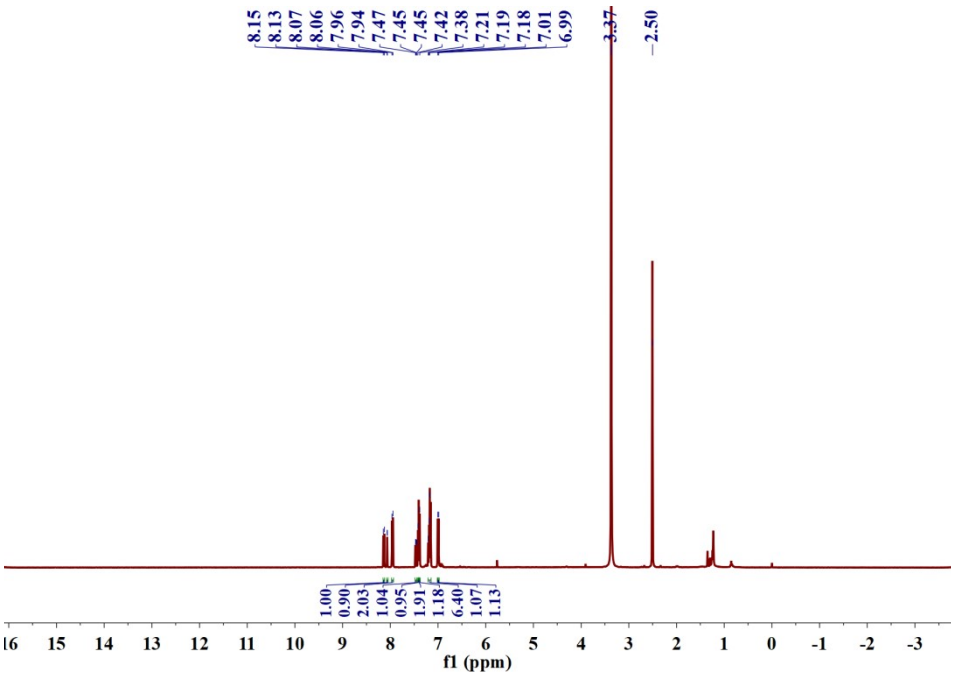

Fig. S36. ^{1}H NMR spectra of 4-(5-chlorobenzo[d]thiazol-2-yl)-N,N-diphenylaniline in DMSO-d_6.

3p. 3-(5-chlorobenzo[d]thiazol-2-yl)phenol (80% yield)

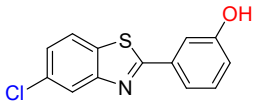

^{1}H NMR (400 MHz, $CDCl_3$) δ 8.04 (d, J = 1.9 Hz, 1H), 7.81 (d, J = 8.5 Hz, 1H), 7.63 - 7.58 (m, 2H), 7.39 - 7.34 (m, 2H), 7.01 (d, J = 7.1 Hz, 1H), 5.65 (s, 1H).

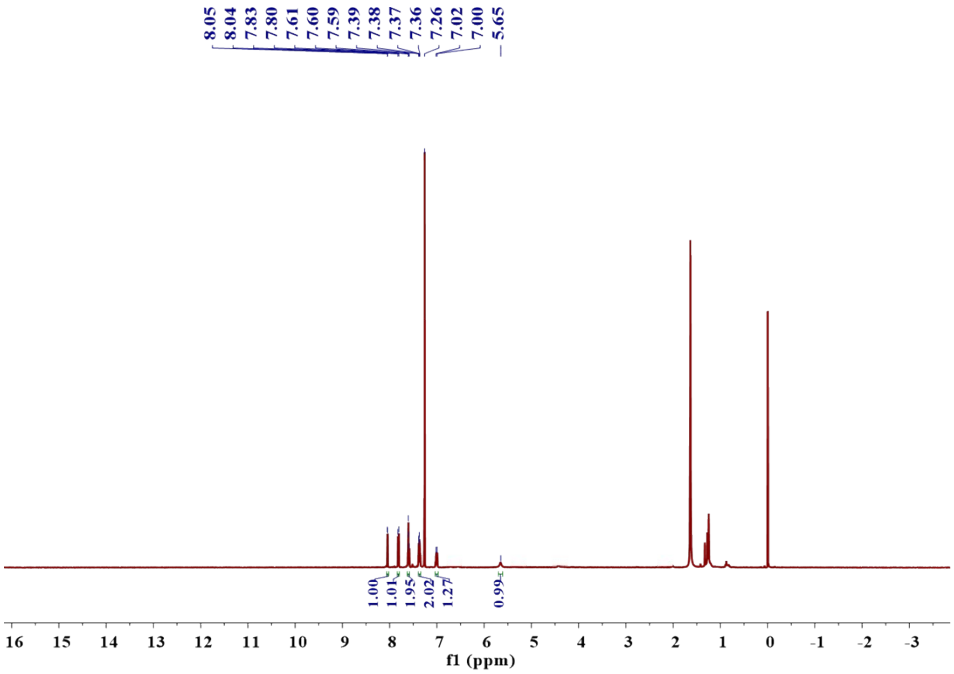

Fig. S37. ^{1}H NMR spectra of 3-(5-chlorobenzo[d]thiazol-2-yl)phenol in $CDCl_3$.

3q. 5-chloro-2-(3,5-dichlorophenyl)benzo[d]thiazole (77% yield)

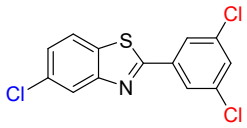

^{1}H NMR (400 MHz, $CDCl_3$) δ 8.03 (d, J = 1.9 Hz, 1H), 7.92 (d, J = 1.8 Hz, 2H), 7.81 (d, J = 8.6 Hz, 1H), 7.46 (t, J = 1.9 Hz, 1H), 7.39 (dd, J = 8.6, 2.0 Hz, 1H).

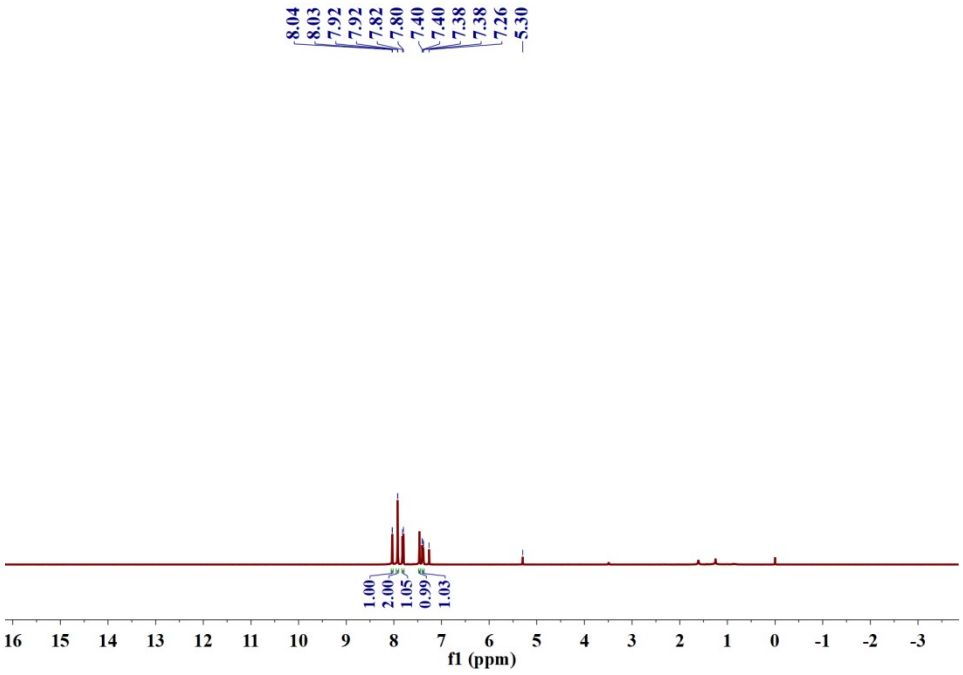

Fig. S38. ^{1}H NMR spectra of 5-chloro-2-(3,5-dichlorophenyl)benzo[d]thiazole in $CDCl_3$.

3r. 5-chloro-2-(3,5-dibromophenyl)benzo[d]thiazole (75% yield)

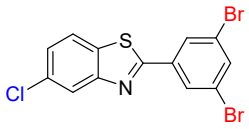

^{1}H NMR (400 MHz, $CDCl_3$) δ 8.17 (d, J = 1.7 Hz, 2H), 8.08 (d, J = 8.2 Hz, 1H), 7.93 (d, J = 7.5 Hz, 1H), 7.77 (t, J = 1.7 Hz, 1H), 7.55 - 7.50 (m, 1H), 7.44 (td, J = 7.7, 1.1 Hz, 1H).

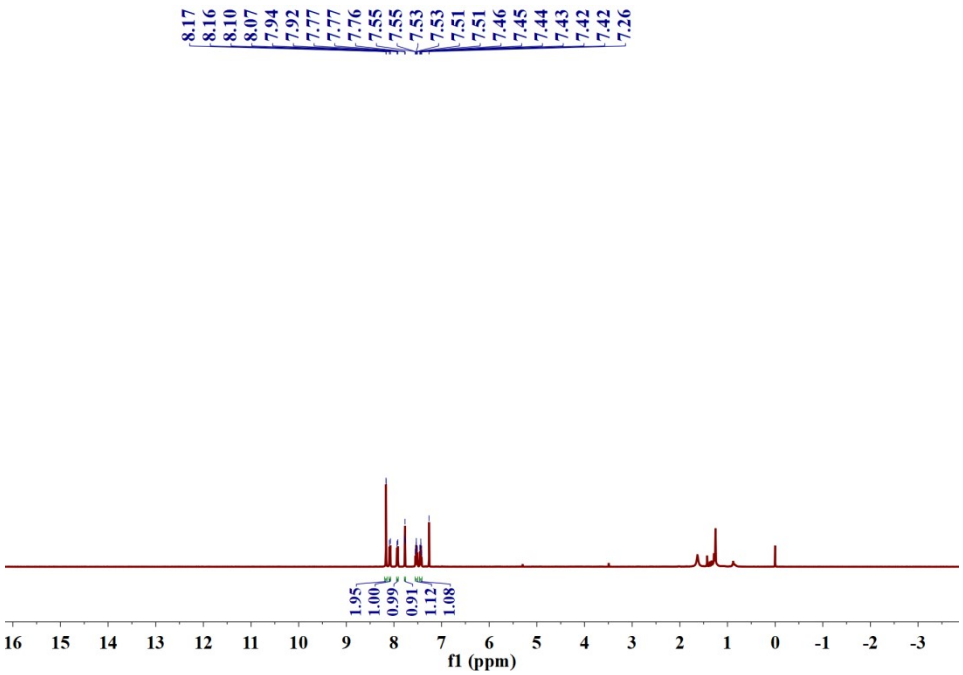

Fig. S39. ^{1}H NMR spectra of 5-chloro-2-(3,5-dibromophenyl)benzo[d]thiazole in $CDCl_3$.

3s. 2-(pyridin-4-yl)benzo[d]thiazole (86% yield)

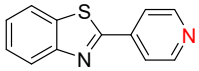

^{1}H NMR (400 MHz, $CDCl_3$) δ 8.78 (d, J = 6.0 Hz, 2H), 8.13 (d, J = 8.5 Hz, 1H), 7.95 (d, J = 6.1 Hz, 3H), 7.59 - 7.52 (m, 1H), 7.49 - 7.43 (m, 1H).

.

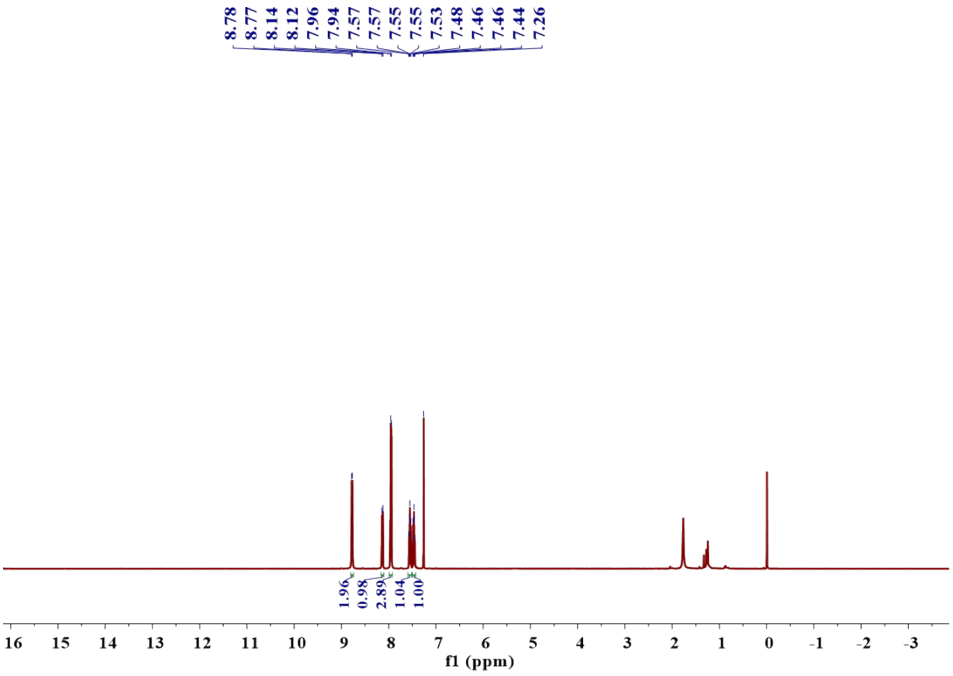

Fig. S40. ^{1}H NMR spectra of 2-(pyridin-4-yl)benzo[d]thiazole in $CDCl_3$.

3t. 2-(thiophen-2-yl)benzo[d]thiazole (95% yield)

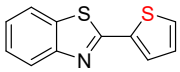

^{1}H NMR (400 MHz, $CDCl_3$) δ 8.03 (d, J = 8.2 Hz, 1H), 7.86 (d, J = 8.0 Hz, 1H), 7.66 (dd, J = 3.7, 1.1 Hz, 1H), 7.53 - 7.44 (m, 2H), 7.40 - 7.34 (m, 1H), 7.14 (dd, J = 5.0, 3.7 Hz, 1H).

.

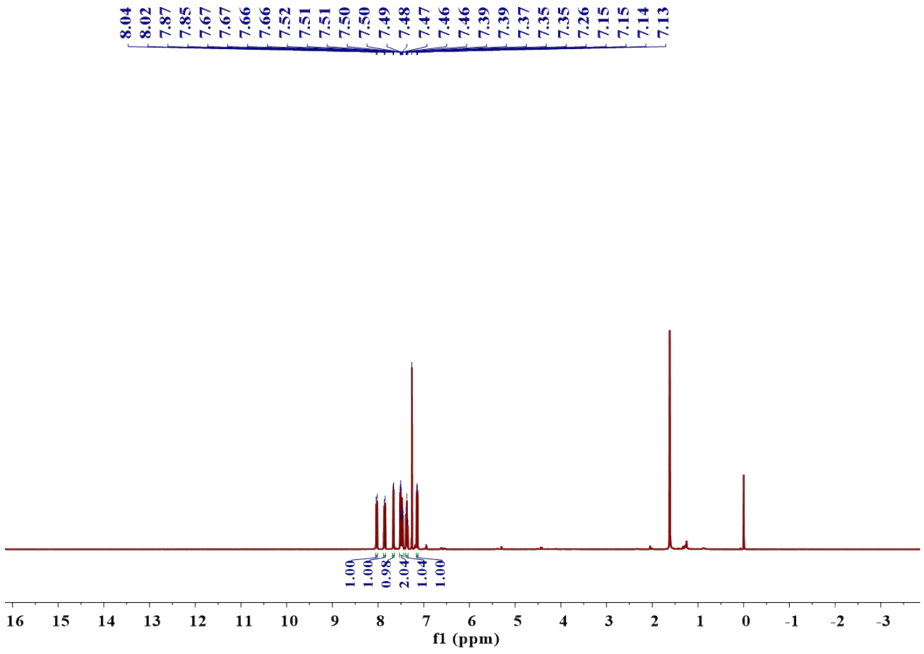

Fig. S41. ^{1}H NMR spectra of 2-(thiophen-2-yl)benzo[d]thiazole in $CDCl_3$.

3u. 2-(furan-2-yl)benzo[d]thiazole (92% yield)

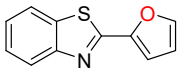

^{1}H NMR (400 MHz, $CDCl_3$) δ 8.05 (d, J = 8.1 Hz, 1H), 7.89 (d, J = 7.8 Hz, 1H), 7.63 - 7.59 (m, 1H), 7.52 - 7.46 (m, 1H), 7.42 - 7.34 (m, 1H), 7.20 (d, J = 3.4 Hz, 1H), 6.60 (dd, J = 3.5, 1.8 Hz, 1H).

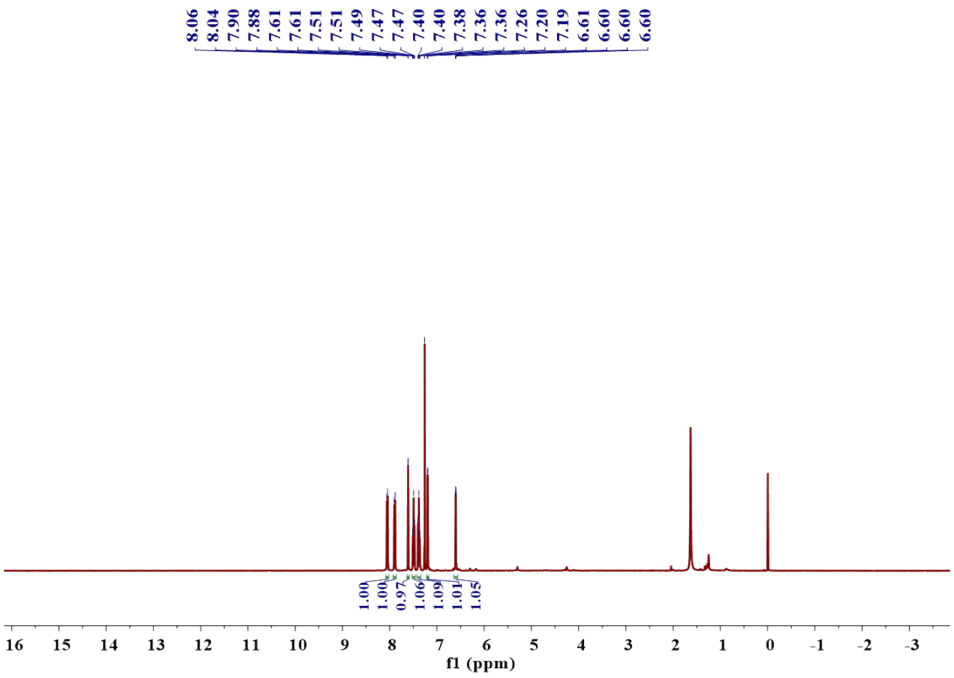

Fig. S42. ^{1}H NMR spectra of 2-(furan-2-yl)benzo[d]thiazole in $CDCl_3$.

3v. benzo[d]thiazole (55% yield)

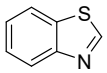

^{1}H NMR (400 MHz, $CDCl_3$) δ 9.00 (s, 1H), 8.15 (d, J = 8.2 Hz, 1H), 7.96 (d, J = 8.0 Hz, 1H), 7.55 – 7.49 (m, 1H), 7.44 (t, J = 7.9 Hz, 1H).

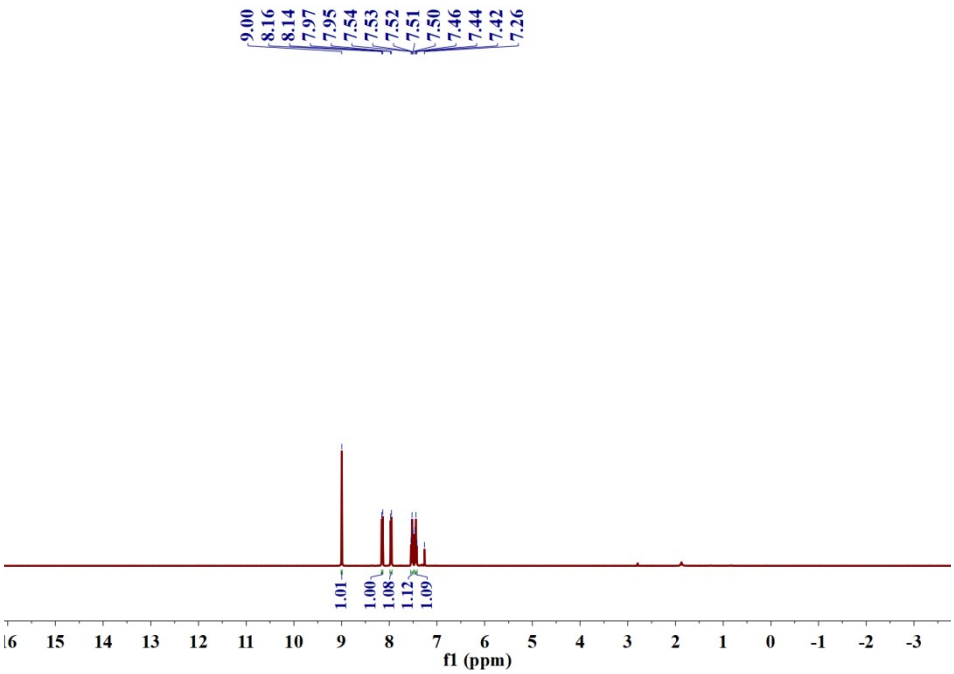

Fig. S43. ^{1}H NMR spectra of benzo[d]thiazole in $CDCl_3$.

3w. 2-ethylbenzo[d]thiazole (52% yield)

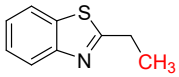

^{1}H NMR (400 MHz, $CDCl_3$) δ 7.97 (d, J = 8.2 Hz, 1H), 7.85 (d, J = 8.1 Hz, 1H), 7.45 (t, J = 7.6 Hz, 1H), 7.35 (t, J = 7.7 Hz, 1H), 3.16 (q, J = 7.5 Hz, 2H), 1.48 (t, J = 7.6 Hz, 3H).

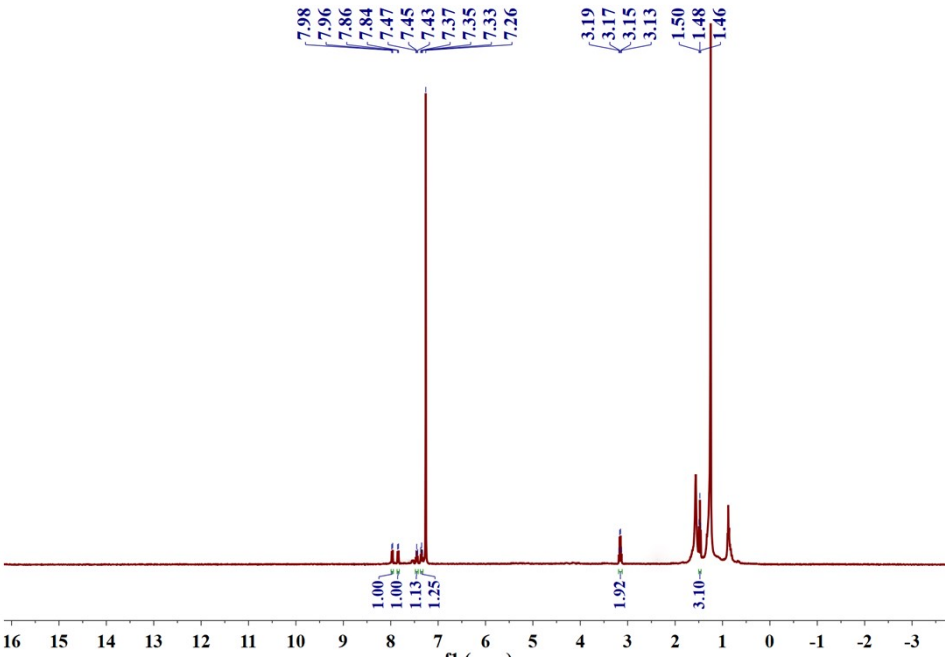

Fig. S44. ^{1}H NMR spectra of 2-ethylbenzo[d]thiazole in $CDCl_3$.

3x. 5-chloro-2-isopropylbenzo[d]thiazole (47% yield)

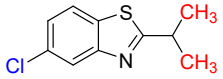

^{1}H NMR (400 MHz, $CDCl_3$) δ 7.96 (s, 1H), 7.75 (d, J = 8.5 Hz, 1H), 7.32 (d, J = 8.5 Hz, 1H), 3.47 - 3.38 (m, 1H), 1.48 (d, J = 6.9 Hz, 6H).

.

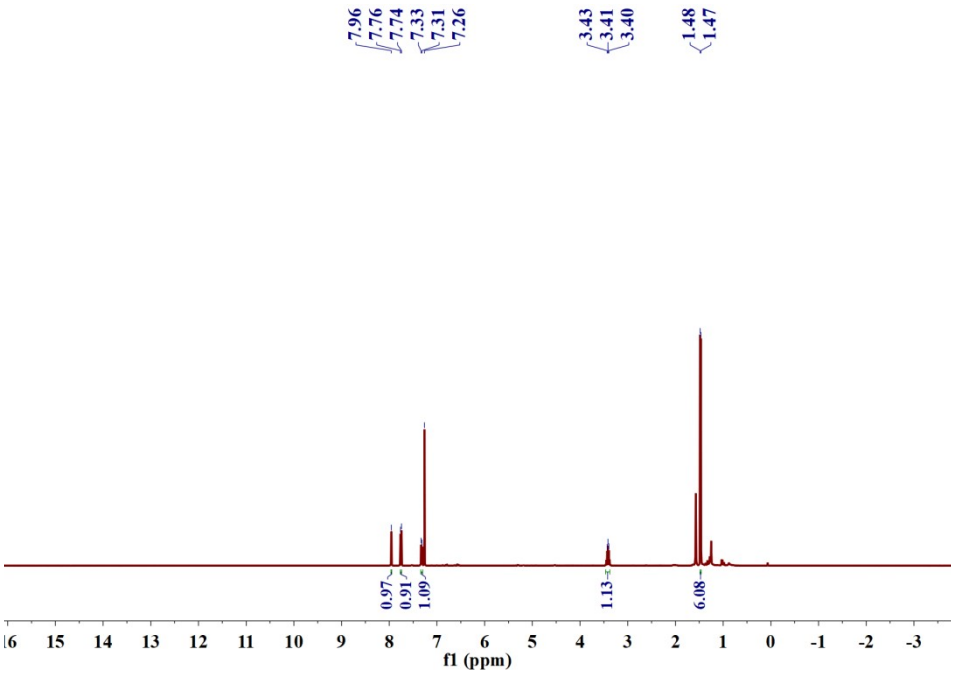

Fig. S45. ^{1}H NMR spectra of 5-chloro-2-isopropylbenzo[d]thiazole in $CDCl_3$.

3y. 2-(pentan-2-yl)benzo[d]thiazole (44% yield)

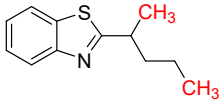

^{1}H NMR (400 MHz, $CDCl_3$) δ 7.97 (d, J = 8.1 Hz, 1H), 7.85 (d, J = 7.9 Hz, 1H), 7.44 (t, J = 7.7 Hz, 1H), 7.34 (t, J = 8.1 Hz, 1H), 3.30 (q, J = 7.0 Hz, 1H), 1.86 (s, 1H), 1.70 (s, 1H), 1.60 (s, 2H), 1.45 (d, J = 6.9 Hz, 3H), 0.93 (t, J = 7.3 Hz, 3H).

.

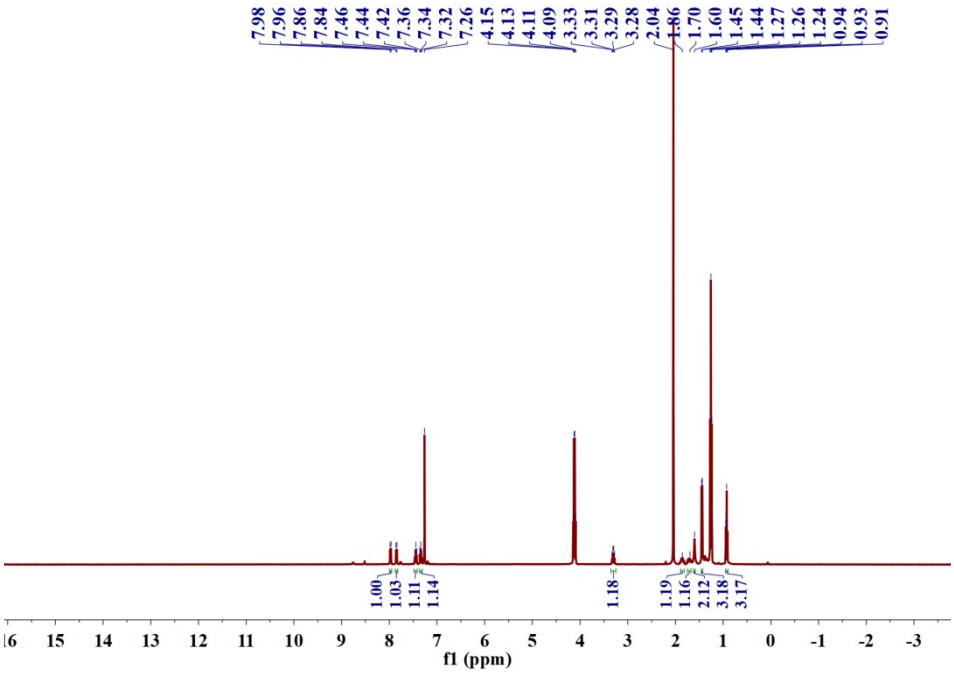

Fig. S46. ^{1}H NMR spectra of 2-(pentan-2-yl)benzo[d]thiazole in $CDCl_3$.